論文 / 著書情報
Article / Book Information

題目(和文)	
Title(English)	Functional analysis of the conserved two component Hik2/Hik34-Rre1 module in a cyanobacterium Synechococcus elongatus PCC 7942
著者(和文)	BairagiNachiketa
Author(English)	Bairagi Nachiketa
出典(和文)	学位:博士(学術), 学位授与機関:東京工業大学, 報告番号:甲第11849号, 授与年月日:2022年3月26日, 学位の種別:課程博士, 審査員:田中 寛,太田 啓之,久堀 徹,和地 正明,増田 真二
Citation(English)	Degree:Doctor (Academic), Conferring organization: Tokyo Institute of Technology, Report number:甲第11849号, Conferred date:2022/3/26, Degree Type:Course doctor, Examiner:,,,,
学位種別(和文)	博士論文
Type(English)	Doctoral Thesis

Functional analysis of the conserved two component Hik2/Hik34-Rre1 module in a cyanobacterium *Synechococcus elongatus* PCC 7942

A dissertation presented by

Nachiketa Bairagi

Academic Supervisor: Kan Tanaka

To

The Department of Life Science and Technology

in partial fulfillment of the requirements

for the degree of

Doctor of Philosophy

In the subject of

Life Science and Technology

Tokyo Institute of Technology

Tokyo, Japan

September 2021

Abstract

Cyanobacteria is a large and morphologically divergent group of oxygenic photosynthetic bacteria found in versatile environmental condition in Earth. Cyanobacteria utilize a unique signal transducing system, namely two component system to sense and respond to environmental changes. Hik2-Rre1 is a multi-stress responsive two-component system that is responsible for the expression of heat shock protein genes in cyanobacteria. In our previous study, heat inducible Rre1 phosphorylation was alleviated in a *hik34* deletion mutant suggesting Hik34 is a positive regulator for the signal. In this study, deletion of *hik34* showed slow growth and alleviation of heat inducible response. After subsequent culture, the mutants restored the growth phenotype as well as heat inducible response, that indicated the acquisition of suppressor mutation. Suppressor mutations were identified in *dnaK2*, *rre1* and *sasA* ORF by whole genome sequencing. Genetic analyses of suppressor mutation in $rre1^{P114L}$ and $sasA^{S83fs}$ showed that the suppressor mutations are epistatic to the phenotypes caused by the *hik34* deletion, and these products are working downstream of Hik34 during the signaling event. These genetic lines of evidence together with the previous reports of Hik2-Rre1 interaction indicated that Rre1 phosphorylation is occurring basically dependent on Hik2 where this phosphorylation event is modulated by Hik34 through the SasA and Rre1 function. A recent study revealed that Hik2 is a redox responsive Fe-S protein and the Hik2 activity is regulated through PQ redox state. Consistently, Rre1 phosphorylation was observed in reduced state of PQ pool, but not under oxidized state of PQ pool, suggesting that the Hik2-to-Rre1 phosphotransfer was activated under PQ reducing condition. Interestingly, *hspA* transcription was induced under oxidized state of PQ pool without the Rre1 phosphorylation that suggests the complexity of the chaperone genes transcriptional regulation. It was also found that, the measured PQ redox status did not correlate with the Rre1 phosphorylation during temperature upshift, and therefore, the heat inducibility was not resulted from changes of PQ redox status.

Meanwhile, 2,6-dichloro-1,4-benzoquinone (DCBQ) dependent oxidation events prevented the heat-inducible Rre1 phosphorylation. It was also found that newly synthesized protein(s) is required to quench the heat induced Hik2-Rre1 response. Based on these results, we finally propose a model for the control of Hik2-dependent Rre1 phosphorylation.

List of figures

List of tables

Supplementary

Acknowledgments

I would like to express my sincere gratitude to my academic supervisor Professor Kan Tanaka for his scholarly advice, continuous support on scientific problem-solving throughout the years. The scholarly vision of Professor Kan Tanaka has helped enormously to grow my thinking as s scientist.

I would like to thank the committee member of my dissertation: Professors Hiroyuki Ohta, Toru Hisabori, Maasaki Wachi and Shinji Masuda for stimulating discussions, for challenging my thinking and helping to improve my research direction. I also thank Drs. Satoru Watanabe, Kaori Nimura-Matsuone, Ken-ya Tanaka and Shuji Nakanishi for their support to accomplish my study. I also wish to thank the members of Tanaka Laboratory for the contribution in my work, sharing thoughts and ideas, and enriching my experience of Tokyo Institute of Technology. I wish to thank MEXT (The Ministry of Education, Culture, Sports, Science and Technology) for supporting my fellowship.

Finally, I would like to thank my Family and Friends for supporting me on this journey, helping me overcome difficulties and sharing times of joy

Chapter 1

Background and Introduction

1.1 Oxygenic Photosynthesis and Cyanobacteria

Evolution of oxygen evolving photosynthesis is one of the major events in the history of life on earth. The atmosphere of the earth was largely anaerobic before the evolution of this metabolic reaction (Doolittle et al. 1996). In the primitive era of earth, there was no eukaryote until the oxygen level rose to a significant level. No other known process, either biogenic or non-biogenic, can originate the large quantities of molecular oxygen that undoubtedly changed the course of life on earth (Blankenship 2010). Oxygenic photosynthesis is considered to have started about 3 billion years ago after ancient cyanobacteria like organisms evolved an apparatus capable of capturing and utilizing solar radiation (300-700 nm). Extracting electrons from H_2O (and reduction of CO_2 to energy-rich carbohydrates) made it possible to release O_2 (Buick 2008). The unique origination of O_2 release and subsequent accumulation in the earth's atmosphere by the first cyanobacteria was undoubtedly the *biological Big Bang* for the evolution of the whole biosphere. Evolution of O_2 created an aerobic condition and background for the development of aerobic metabolism and forms more advanced life on the earth (Olson et al. 2005). Alongside evolution of O_2 in atmosphere, cyanobacteria also originated the event of *endosymbiosis* (Archibald 2009). Cyanobacteria are the photosynthetic ancestors of plastids in algae and higher plants (Bhattacharya et al. 2004, Waterbury et al. 1979).

Cyanobacteria (formerly classified as "blue-green algae") are one of the largest and versatile groups of prokaryotes, producing about 20%-30% of global photosynthetic activity (Field et al. 1998). This corresponds to fixation of CO_2 about 20-30 Gt into biomass and release of 50-80 Gt of O_2 yearly in the atmosphere by these oxygenic prokaryotes. Cyanobacteria can fix N_2 into a biologically accessible form play an important role in nitrogen cycle of biosphere Cyanobacteria are highly versatile as they exhibit wide ecological tolerance and can be found in almost any environment (e.g., benthos, plankton, cold and hot deserts, Antarctic dry valleys, tropical rain forests) (Cohen et al. 1986). Most of the cyanobacteria can perform oxygenic

photosynthesis beside some are able to grow as anaerobic photoautotrophs using H_2S as electron donor. This signifies unique capability of anoxygenic photosynthesis in these organisms, while those couldn't be able to utilize H_2O as substrate and produce O_2 (Robinwitch 1960).

The mechanism of oxygenic photosynthesis in cyanobacteria highly resembles that of oxygenic higher plants and algae. This similarity allows to use cyanobacteria as a suitable model to study different aspects of oxygenic photosynthesis and its regulation that is often difficult to study in higher plants or algae. Cyanobacteria share the use of unique reaction centers (RCs), P680 and P700, to drive light induced electron transfer from H_2O to $NADP^+$ (Nicotinamide adenine dinucleotide phosphate); its reduced form NADPH, is used to power the synthesis of carbohydrates like photosynthetic higher organisms. Like higher plants and algae, cyanobacteria have two photosystems (PSs) that work in series which was known from the Emerson's enhancement effect experiments and form antagonistic effects of light I (absorbed by PSI) and light II (absorbed by PSII) on electron transfer.

Cyanobacteria contain photosynthetic pigment chlorophyll (Chl) like other oxygenic photosynthesizers. Carotenoids (Cars) and phycobilins are found in most cyanobacteria, though phycobilins are absent in higher plants. Phycobilins are organized in large light harvesting multiprotein complexes called phycobilisomes (PBSs) in cyanobacteria (Kurisu et al. 2003).

Cyanobacterial cells surrounded by two membranes: inner one, the cytoplasmic membrane, which separates the cytoplasm from the periplasm and outer one, which protects the cell wall (Figure 1.1). The light dependent oxygenic photosynthesis takes place in thylakoid membranes. The closed compartment in thylakoid membrane is called thylakoid lumen. In cyanobacteria, respiration and photosynthesis redox active protein complexes share a common thylakoid membrane, as not found in higher plants. The thylakoid membrane in cyanobacteria

doesn't form grana as it does in plants and algae. In all oxygenic organisms, light driven electron transport oxidizes H_2O and results in evolution of O_2, reduces $NADP^+$ to NADPH and phosphorylates ADP to ATP (Figure 1.2). Cyanobacteria can live almost any condition on the earth which suggests they have some mechanisms to acclimate themselves in extreme conditions. To inhabit and survive diverse environmental conditions, cyanobacteria rely on a signal transduction system, "two component system (TCS)", a versatile environmental sensing and signal transduction system that modulates gene expression for acclimation.

1.2 Two Component System

In response to various environmental conditions, bacteria and other organisms including cyanobacteria rely on versatile environment sensing and signal transduction systems that modulate gene expression for acclimation. The signal transduction module generally found in bacteria are two component systems (TCS), serves as basic stimulus-response to sense and respond to environmental changes (Stock et al. 2000). Two component systems are basically composed of membrane bound histidine kinases (HKs) that sense specific signal of environment change and response regulators (RRs) that mediate cellular response through expression of target genes (Mascher et al. 2006). The HKs contain a sensing domain and a Hik domain as the basic structure, and a conserved histidine residue in Hik domain is auto-phosphorylated in response to some environmental changes. Auto-phosphorylation of HKs trigger transfer of phosphoryl group to a conserved aspartate residue in the receiver domain of cognate RRs. Subsequently, RRs change the conformation which stimulate binding of the RRs to specific DNA sequence and activate or repress the regulatory target genes (Mascher et al. 2006). (Figure 1.3)

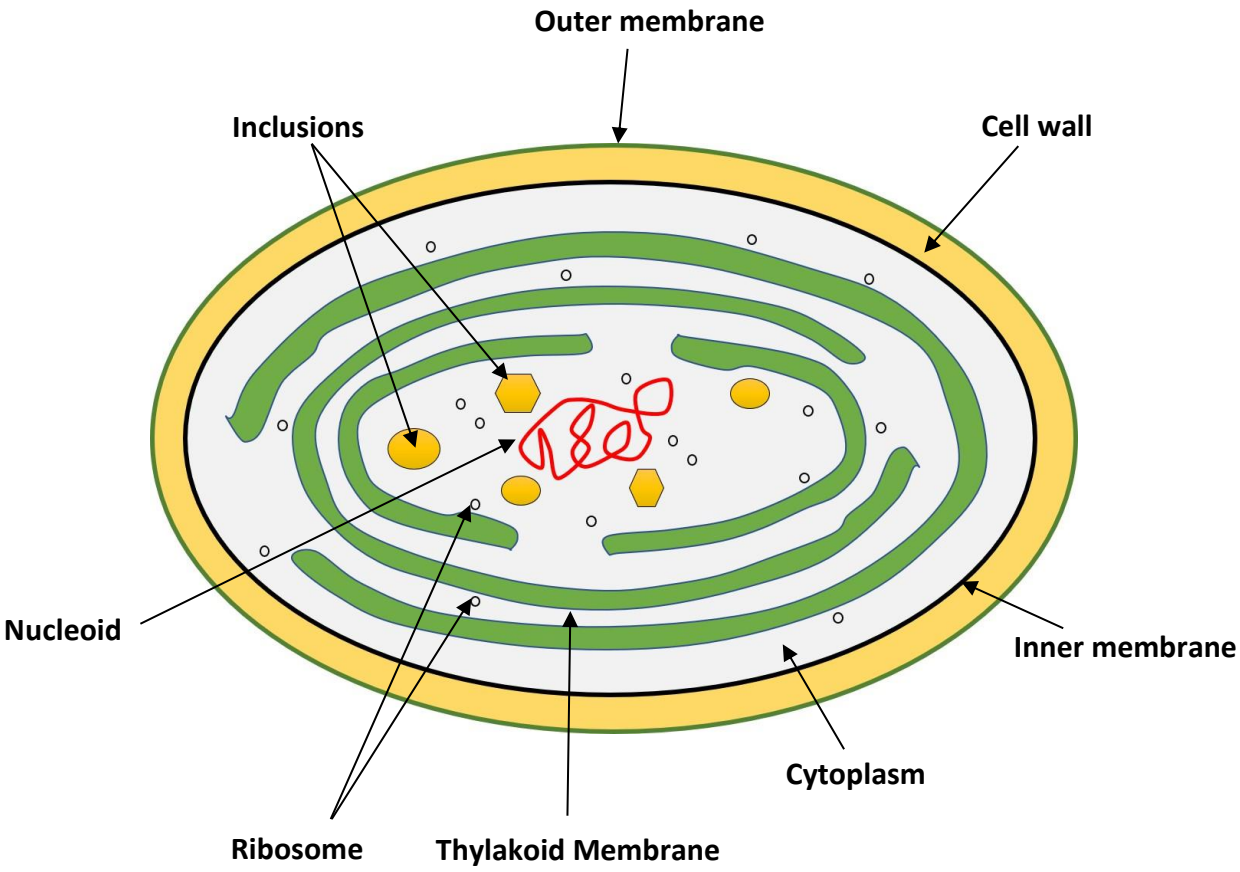

Figure 1.1(see color insert) A schematic outline of a cyanobacterial cell.

The thylakoid membranes (green) contain chlorophyll and perform both photosynthetic and respiratory electron transport. While inner membrane (black) contains carotenoids, is involved only in respiration. During photosynthetic and respiratory transport system, protons are brought into the thylakoid lumen, the space between thylakoid membranes. This proton gradients are utilized for the synthesis of ATP. (Modified and adapted from Vermass, W.F.J., *Encyclopedia of Life Science (ELS)*, John Wiley and Sons, Ltd, London, U.K., 2001. Copyright Wiley-VCH Verlog GmbH and Co. KGaA)

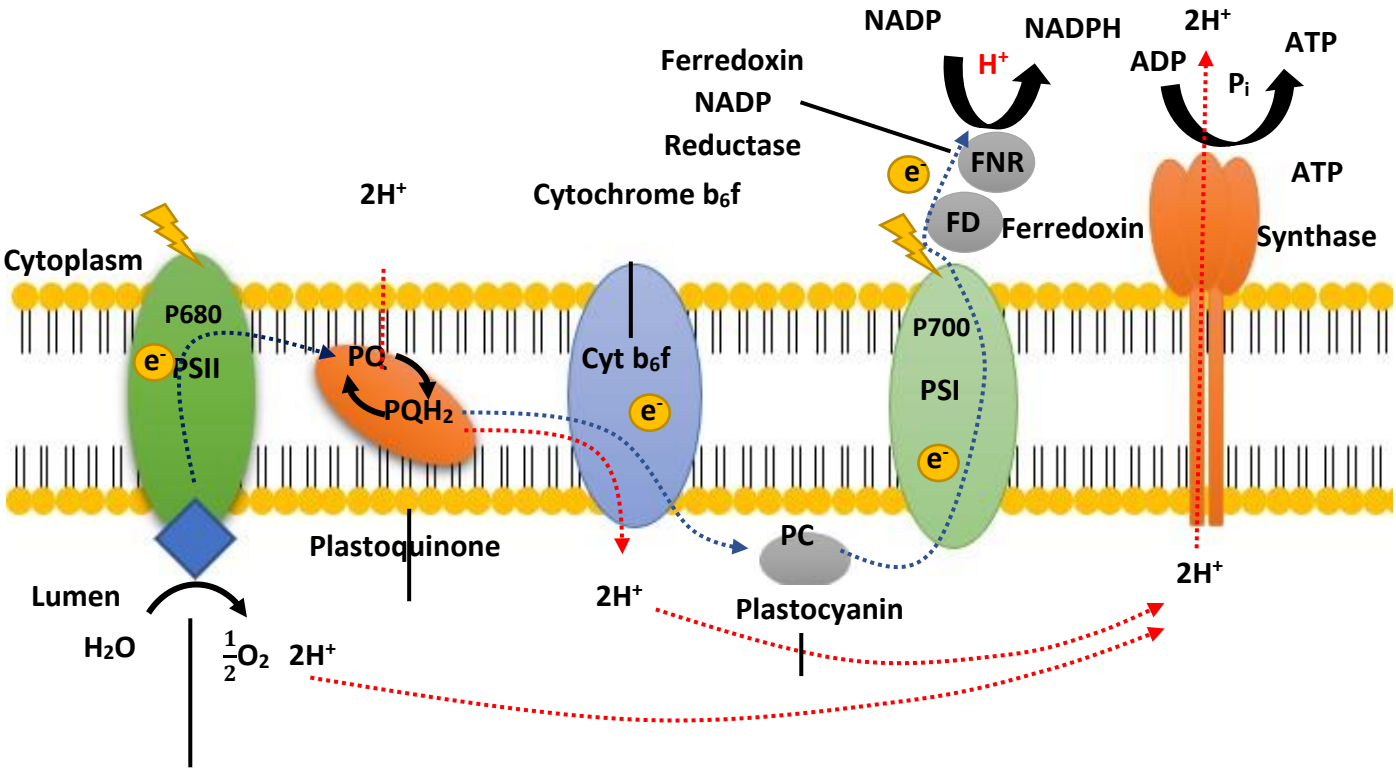

Figure 1.2 (see color insert) A schematic representation of light induced electron and proton transfer reactions of oxygenic photosynthesis of cyanobacteria.

The blue arrows indicating the light-driven electron transfer and the red arrows indicating the dark reactions as shown in the figure. The abbreviated components from the left of the diagram: PSII, photosystem II; PQ, plastoquinone; PQH_2, plastoquinol; Cyt b_6f, cytochrome b_6f; PC, plastocyanin; PSI, photosystem I; Fd, ferredoxin; FNR, ferredoxin-NADP reductase. In the light-dependent reactions, one molecule of the pigment chlorophyll absorbs one photon and loses one electron. This electron is passed to a modified form of chlorophyll called pheophytin, which passes the electron to first Q_A then to plastoquinone pool, starting the flow of electrons down an electron transport chain that leads to the ultimate reduction of NADP to NADPH. In addition, this creates a proton gradient across the chloroplast membrane, which is used by ATP synthase in the synthesis of ATP.

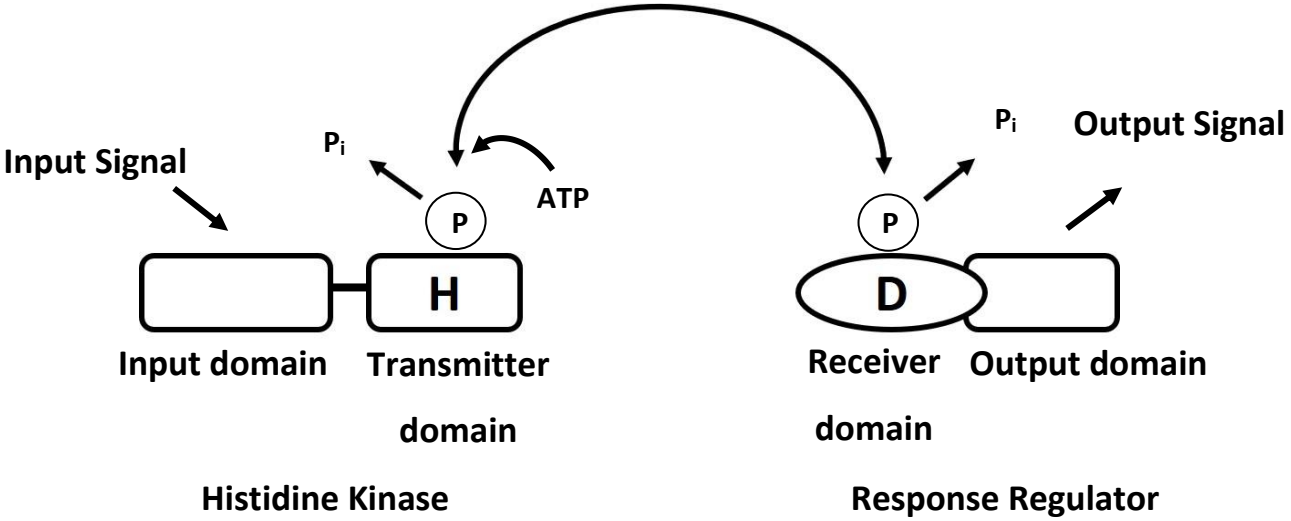

Figure 1.3 General model of Two Component System

Two-component systems accomplish signal transduction through the phosphorylation of a response regulator (RR) by a histidine kinase (HK). Upon detecting a particular change in the extracellular environment, the HK performs an autophosphorylation reaction, transferring a phosphoryl group from adenosine triphosphate (ATP) to a specific histidine residue. The cognate response regulator (RR) then catalyzes the transfer of the phosphoryl group to an aspartate residue on the response regulator's receiver domain. (Modified and adopted from Mähönen, Ari Pekka. "Cytokinin's regulate vascular morphogenesis in the *Arabidopsis thaliana* root, 2005).

1.3 Cyanobacterial Two Component System

The cyanobacteria constitute a very large and morphologically divergent group of oxygenic photosynthetic prokaryotes. In almost all environments including terrestrial, freshwater and marine habitats, cyanobacteria can be found. Like most bacteria, cyanobacteria use two component system (TCS) to regulate cell behavior and gene expression in response to changes in the external environment (Marine et al. 2003). A number of TCS genes were revealed in bacterial genomes by whole genome sequence. Pairs of HK and RR genes that function uniformly are often located to next to each other. The relationship between HK and RR modulates specific signal transduction pathways. Genome sequences of the cyanobacteria have revealed that they have variety of TCS proteins to regulate responses to the environment. Total 85 completely sequenced cyanobacterial genome are available in Cyanobase (www.genome.microbedb.jp/cyanobase/). Available genomes come from unicellular and filamentous freshwater or terrestrial strains and from marine environments. The extensive analysis of TCS proteins in each organism opened up the secret of survival of cyanobacteria in variable environments (in each of the cyanobacterial strain, genes encoding components of TCSs were typically found).

Functional analyses of TCS proteins have been performed mainly in the model cyanobacteria *Synechococcus elongatus* PCC 7942 (hereafter referred as *S. elongatus*) and *Synechocystis* sp. strain PCC 6803 (hereafter referred as *Synechocystis*). In this study, I analyzed function and regulation of TCS components in *S. elongatus* in various environmental conditions. From the orthologous clustering analysis of TCS proteins among all cyanobacteria, it is indicated only four HKs (Hik2, Hik34, NblS and SasA) and three RRs (RpaA, RpaB and Rre1) were almost perfectly conserved in all sequenced cyanobacterial strains (Rubin et al. 2015, Ashby et al. 2006). These highly conserved TCS proteins notably play critical roles in central signaling system of sensing environmental changes and acclimation processes in

cyanobacteria. Among the perfectly conserved TCS proteins, Hik2, NblS, RpaB and Rre1 are essential for viability in cyanobacteria (Rubin et al. 2015, Ashby et al. 2006). These essential TCS proteins are also found broadly, even in red and other algal chloroplasts that originated from cyanobacterial endosymbiont (Hanaoka et al. 2010).

1.4 Conserved Two Component System in Cyanobacteria

SasA and RpaA are well known TCS for the circadian rhythm regulation, where SasA activity is modulated under the control of the clock Kai complex and RpaA propagates the time information onto the genome wide transcriptome changes (Iwasaki et al. 2000, Takai et al. 2006). The TCS composed of NblS and RpaB is responsible for the genes activation responding to diverged stressed conditions, such as high light, cold temperature, high salt and high osmolarity (Kappell and van Waasbergen 2007, Hanaoka and Tanaka 2008, Moronta-Barrios et al. 2012). While the remaining three modules, Hik2, Hik34 and Rre1, have been suggested to involve in multiple stress responses as well (Paithoonrangsarid et al. 2004, Shoumskaya et al. 2005), the detailed functional analyses have been initiated only recently because of the complicated signaling events interacted with other modules. Hik2, NblS, RpaB and Rre1 are essential for viability (Rubin et al. 2015, Ashby and Houmard 2006), which is also making difficulty in the functional analysis

1.5 Hik2-Rre1 Modulation in cyanobacterial stress response

Lines of evidence for the Hik2-Rre1 TCS module have been obtained. Firstly, Hik2-Rre1 specific interaction was shown in a yeast two-hybrid assay in *S. elongatus* (Sato et al. 2007, Kato et al. 2012). Secondly, *in vitro* phosphor-transfer analysis revealed that Hik2 could phosphorylate Rre1 using *S. elongatus* and *Synechocystis* proteins (Kato et al. 2012, Vidal et al. 2009, Ibrahim et al. 2016). Recent biochemical analysis revealed that Hik2 of *Synechocystis* is an iron-sulfur protein containing a highly redox responsive [3Fe-4S] (Ibrahim et al. 2020).

The *Synechocystis* Hik2 protein contains a GAF domain likely sensing environmental changes, and a conserved cysteine residue near the N-terminus of the GAF domain was involved in the assembly of the Fe-S cluster. It was proposed that Hik2 is activated under PQ oxidizing conditions which is mediated by [3Fe-4S] cluster attached with the conserved GAF domain (Ibrahim et al. 2020). Meanwhile, comparison of Hik2 proteins predicted from sequenced genome sequences found that some Hik2 proteins, including of *S. elongatus*, lacks the conserved cysteine residue in their GAF domain (Ibrahim et al. 2020). Thus, universality of the Hik2 sensing mechanism remained elusive.

1.6 Hik34-Rre1 modulation in cyanobacterial stress response

For the Rre1 functional analysis, we previously performed ChIP-on-chip (chromatin immunoprecipitation mapping on tiling array) analysis for the genome-wide identification of the Rre1 binding sites (Kobayashi et al. 2017). The results revealed that Rre1 can bind to promoter regions of major chaperone protein genes such as *dnaK2, groESL-1, groEL-2, hspA* and *htpG,* as well as the group 2 sigma factor *rpoD2* after high temperature upshifts. Rre1 was phosphorylated as correlated with the downstream transcriptional activation under these conditions, and thus it was concluded that Rre1 is the transcription factor that is responsible for the heat shock inducible transcription of major chaperone genes. While it was difficult to show the Hik2 involvement because the *hik2* gene is essential, we found the heat inducible response was diminished in a knock-out mutant of Hik34, which is another histidine kinase previously suggested to involve heat shock response in *Synechocystis* (Suzuki et al. 2005). These results led us to the conclusion that Hik34 rather than Hik2 is likely predominantly responsible for the heat inducible transcriptional activation mediated by Rre1 (Kobayashi et al. 2017).

Notwithstanding, it appears to be contradictory that thus far no evidence has been obtained for direct interaction and phosphotransfer between Hik34 and Rre1 (Sato et al. 2007, Kato et al. 2012). Hik34 is a highly conserved histidine kinase and has been considered to control the expression of chaperone protein genes under the salt and hyperosmotic stress based on microarray analyses using *hik34* knock-out mutants in *Synechocystis* (Paithoonrangsarid et al. 2004, Shoumskaya et al. 2005). Other analyses showed that expression of heat shock induction of chaperon and other protein genes was variously affected in a *hik34* mutant in *Synechocystis* (Suzuki et al. 2005, Slabas et al. 2006). However, interrelationship among these three TCS modules remains to be examined.

In this study, mutant analyses revealed that dependence of the heat shock response on Hik34 was negated by secondary mutations, indicating that the Rre1 phosphorylation event was occurring dependent on Hik2 but not Hik34. Our subsequent results suggested both redox-dependent and heat shock-dependent events are involved in the Hik2 activity modulation in an independent but interconnected manner. We also show evidence for the Hik2 inactivating signaling pathway as well as the complexity of the chaperone protein genes transcriptional regulation.

Chapter 2

Secondary mutations suppressed slowed growth and alleviated heat shock response phenotypes of a *hik34* deletion

2.1 Introduction

In our previous study, it is found that heat inducible Rre1 phosphorylation and *hspA* transcription was much diminished in a knock-out mutant of Hik34, which is a conserved histidine kinase previously suggested to be involved in heat shock response in *Synechocystis* (Suzuki et al. 2005). The result suggested that Hik34 could be predominantly responsible for the heat inducible transcriptional activation mediated by Rre1 (Kobayashi et al. 2017). The interaction between Hik34 and Rre1 hasn't obtained, and there is no evidence of phosphotransfer between Hik34 and Rre1 (Sato et al. 2007, Kato et al. 2012). In this study, it was shown that heat inducible Rre1 phosphorylation and downstream gene transcription are independent of Hik34 by a line of genetic evidence.

2.2 Materials and Methods

2.2.1 Bacterial strains, culture media and mutant strain constructions

S. elongatus (WT) and its mutants were grown in BG-11 (Rippka 1988) liquid medium (2% CO_2 aeration) or BG-11 solid medium containing 1.5% w/v agar at 30^{o}C under continuous fluorescent light (30 µmol photons/m^2/s). BG-11 medium and plates were supplemented with 40 µg/ml spectinomycin or 10 µg/ml kanamycin as per requirement. Cultures were grown to OD_{750}=0.5 in BG-11 liquid medium for to examine in several condition. Temperature upshift experiments were performed by transfer the culture media to water bath (45°C) placed in the same incubation condition mentioned above.

2.2.2 Reconstruction of *hik34* deletion mutant

hik34-F and hik34-R primers were used to amplify the *hik34*::Km cassette by PCR reaction from the previously constructed *hik34* deletion mutant strain (Kobayashi et al., 2017) and used to transform the WT *S. elongatus*.

2.2.3 Genome sequencing of cyanobacterial strains

Genomic DNA was extracted from cyanobacterial cells as described (Kirby, K.S. et al. 1967) with some modification. The purity of the genomic DNA extract was determined using a Nano-drop 2000C (Thermo Fischer Scientific, Inc., Waltham, MA, USA). Genomic DNA (600 ng) was fragmented to an average length of 500 bp using a Covaris S2 sonication system (Covaris, Inc., MA, USA). Sequencing libraries were prepared using the NEBNext Ultra DNA Library Prep Kit for Illumina (New England Biolabs). Paired-end sequencing was carried out for 300 cycles using the MiSeq system (Illumina Inc., CA, USA) according to the manufacturer's specifications. The sequencing reads were trimmed using CLC Genomics Workbench ver. 9.5.4 (Qiagen, Venlo, Netherland) with the following parameters: Phred quality score > 30; removing the terminal 20 nucleotides from the 5′ end and 5 nucleotides from 3′ end; and removing truncated reads <30 nucleotides in length. Trimmed reads were mapped to the reference genome sequence and plasmids of *S. elongatus* (accession number: NC_007604) using CLC Genomics Workbench ver. 9.5.4 (Qiagen) with the following parameters: length fraction: 0.8, and similarity fraction: 0.9. To identify SNPs and indels, we used the filter settings as follows: minimum read depth for SNP/indel calling, 20; minimum read depth for the SNP calling, 10; and an 80% cutoff of percent aligned reads calling the SNP per total mapped reads at the SNP sites. Original sequence reads were deposited to the DRA/SRA database with the following accession numbers (DRX296685-DRX296692).

2.2.4 Genetic analysis of *rre1*^{P114L} mutation.

The *rre1*^{P114L} ORF and the 3'-downstream DNA sequence were amplified from SU94 by PCR using DNA primer sets [rre1-Fw-NotI and rre1-Rv-BamHI] and [rre1DN-Fw-XhoI and rre1DN-RV-KpnI], respectively. These fragments were inserted into both side of the spectinomycin resistance gene of pBΩH (Hasegawa et al. 2020) by standard procedures using restriction enzyme digestion and ligation. The resultant plasmid was transformed to WT for the spectinomycin resistance, and *rre1*^{P114L} containing transformants were screened by direct genome sequencing to obtain R94. Subsequently, the *hik34*::Km DNA cassette were transformed to obtain RH94. The primers were listed in Table. S2.

2.2.4 Genetic analysis of *sasA*^{S83fs} mutation.

The *sasA*^{S83fs} ORF and the 3'-downstream DNA sequence were amplified from SU103 by PCR using DNA primer sets [sasAUp-F-SacI and sasA-Rv-NotI] and [sasADN-FW-XhoI and sasADN-RV-KpnI], respectively. These fragments were inserted into both side of the spectinomycin resistance gene of pBΩH by standard procedures using restriction enzyme digestion and ligation. The resultant plasmid was transformed to WT for the spectinomycin resistance, and *sasA*^{S83fs} containing transformants were screened by direct genome sequencing to obtain S103. Subsequently, the *hik34*::Km DNA cassette were transformed to obtain SH103. The primers were listed in Table. S2.

2.2.5 Genetic analysis of *dnaK*^{R408C} mutation.

The *dnaK*^{R408C} ORF and the 3'-downstream DNA sequence were amplified from SU92 by PCR using DNA primer sets [dnaK2-Fw-SacI and dnaK2-Rv-BamHI-SmaI] and [2469-Fw-SalI and 2469-Rv-KpnI], respectively. These fragments were inserted into both side of the spectinomycin resistance gene of pBΩH by standard procedures using restriction enzyme digestion and ligation. The resultant plasmid was transformed to WT for the spectinomycin

resistance, and *dnaK2*^{R480C} containing transformants were screened by direct genome sequencing. However, no transformant containing *dnaK*^{R408C} was obtained. The primers were listed in Table. S2.

2.2.6 RNA analysis

Cells were harvested from the culture tubes after each experimental time point and collected using centrifugation (7000 × g, 2 m, 4^{o}C) and stored at -80^{o}C for further analysis. Total RNA was extracted from the *S. elongatus* cells using hot phenol method (Mironov, K.S., Los, D.A. 2015) and 3 µg of total RNA were used for the northern hybridization analysis (Seki et al. 2007). For *hspA* probe preparation, the following primers were used to amply the *hspA* DNA fragment: hspA-Prb-Fw and hspA-Prb-Rw. Digoxigenin deoxyribonucleoside triphosphate (DIG dNTPs) (DIG DNA labelling mix, Roche, Basel, Switzerland) were labelled with the DNA by PCR reaction. The primers used for the probe amplification were listed in Table. S2.

2.2.7 **Immunoblot and Phos-tag SDS-PAGE analyses**

Details method of Phos-Tag SDS-PAGE is described at the supplemental section. (Modified from Kim et al. 2015)

2.3 Result

2.3.1 Secondary mutations suppressed slowed growth phenotypes of a *hik34* deletion

It was previously shown that Rre1 phosphorylation and the resultant transcriptional activation of chaperone protein genes under temperature upshift was much alleviated in a *hik34* deletion mutant (Kobayashi et al. 2017). After this study, it was noticed that the *hik34* mutant was slow at growth as compared with the parental strain and easily lose the viability during the prolonged storages. To confirm such phenotypes of the mutant, the *hik34* gene region of the mutant containing the kanamycin resistance gene was PCR amplified from the first mutant and used to transform the wild-type (WT) strain to reconstruct the *hik34* mutant (NB34) (Fig. 2.1). Complete segregation of the *hik34* gene deletion and the slow growth was again observed for NB34 (Fig. 2.2). Subsequently, during the cultivation of NB34 on agar plates, we noticed the appearance of colonies that resumed the growth rate as comparable with WT, which could be stably isolated as independent clones. We considered that the occurrence of unknown mutation(s) suppressed the slow growth phenotype resulted from the *hik34* mutation, and further analyzed these strains in this study.

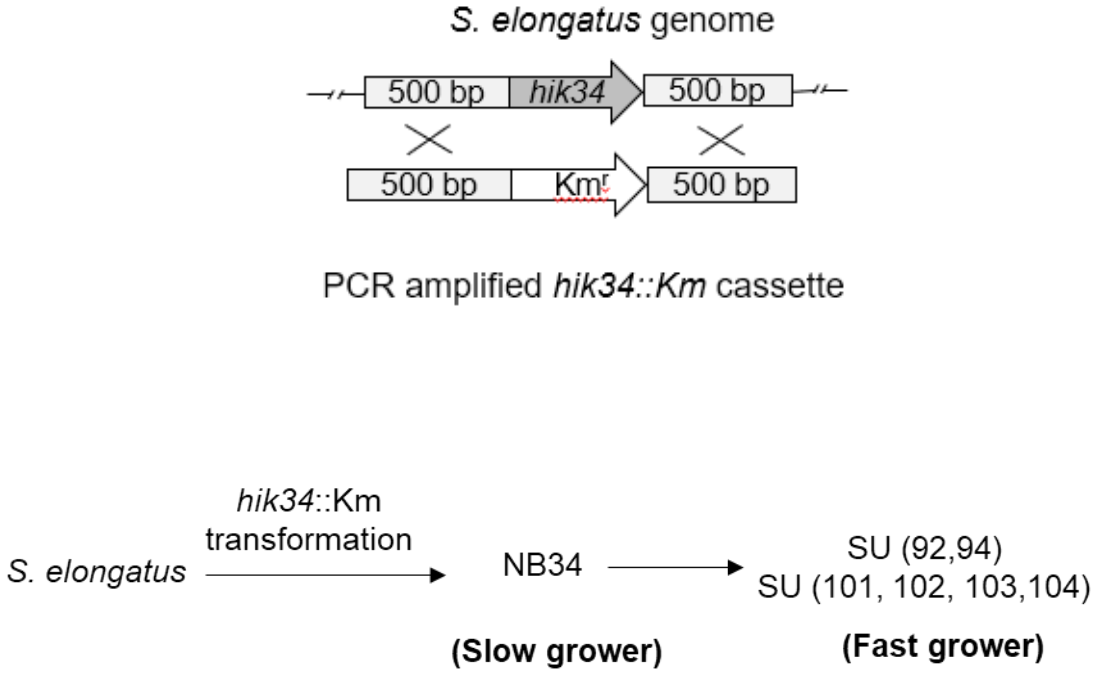

Fig. 2.1 Scheme of *hik34* deletion mutant construction and suppressor mutant isolation. hik34-F and hik34-R primers were used to amplify the *hik34*::Km cassette from the previously constructed hik34 deletion mutant strain (Kobayashi et al., 2017) and used to transform the WT *S. elongatus*. The firstly obtained transformant NB34 resulted in the occurrence of suppressor mutant strains (SU strains).

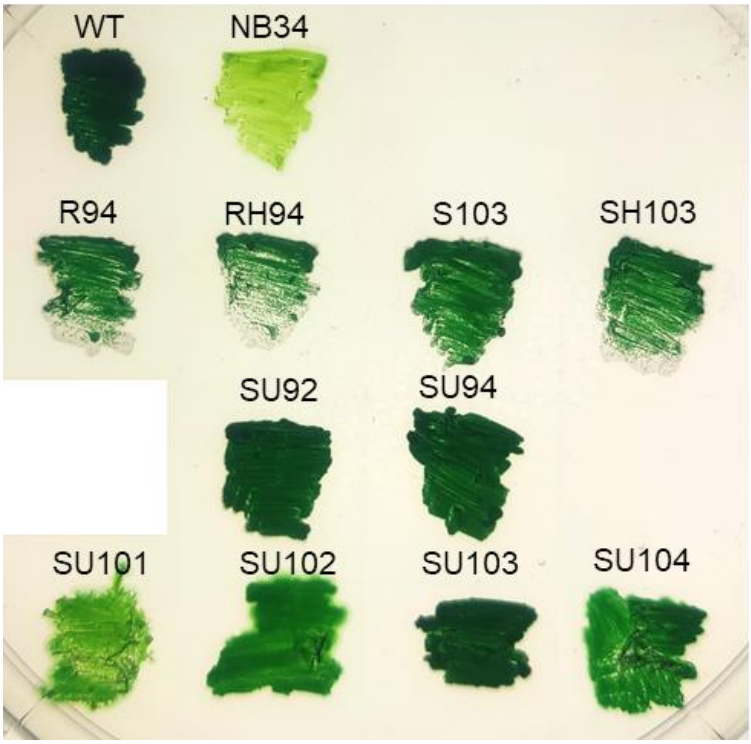

Fig. 2.2 Cell growth of *hik34* deletion mutants.

2.3.2 Identification of suppressor mutation in *hik34* deletion mutants

Starting from NB34, six independently emerged strains, SU92, SU94, SU101, SU102, SU103 and SU104, showing the recovered growth rate were isolated (Fig. 2.2), and subjected to the whole genome sequencing analysis together with the parental WT strain to identify the suppressing mutations. Summary of the results are shown in Table 1. As compared with the *S. elongatus* genome sequence deposited in the database (https://www.ncbi.nlm.nih.gov/genome/?term=Synechococcus%20elongatus%20PCC%207942), the genome sequence of the parental WT strain differed at 8 loci (Shown in gray in Table 1) and these differences were commonly found from the obtained six suppressor strains. Thus, these base changes were already present in WT and not relevant to the newly acquired *hik34* deletion suppressor mutation. Six additional sequence differences were found from all of suppressor strains but not from the parental WT strain. Because the resumed growth suppressor strains emerged from the slow growing NB34 independently, these common six loci are unlikely the reason for the relevant suppression. From the remaining sequence differences, we firstly chose two candidate genes relevant to the suppression, *rre1* (synpcc7942_1860) and *sasA* (synpcc7942_2114), as possible unique candidate mutation in these genes were found in SU94 and SU103, respectively. As another candidate gene for further analysis, we chose a *dnaK2* (synpcc7942_2468) mutation found in SU92. While another mutation was found in SU92 in synpcc7942_1677, the identical base change was found in SU102 and SU104 as well, and therefore this mutation was unlikely resulted in the suppression because actual suppression mutations were likely occurred independently at the final stage after this mutation.

Strain	Location	Nucleic acid substitution	Locus_tag (NC_007604 (CDS))	Gene position, direction	Amino acid change
NB34	92978	T to C	Synpcc7942_0095	92,590-93,339, Complement	Gln121Arg
	711285	G to T			
	759963	G to T			
	769834	C to A	Synpcc7942_0778	769,574-770,038, Direct	
	862420	G to T	Synpcc7942_0859	860,118-862,976, Direct	Arg768Leu
	924962	T to C	Synpcc7942_0918	924,079-926,028, Direct	Leu295Pro
	985854	T to C	Synpcc7942_0977	985,009-986,010, Complement	Lys53Glu
	1052710	T to C	Synpcc7942_1037	1,051,311-1,053,254, Direct	Met467Thr
	1560734	G to A	Synpcc7942_1510	1,560,399-1,561,178, Complement	Gln149*
	1568316 to 1568317	Insertion A			
	2026943	A to G	Synpcc7942_1954	2,026,183-2,027,823, Complement	Val294Ala
	2195908	G to T	Synpcc7942_2114 (*sasA*)	2,194,827-2,195,990, Direct	Arg361Leu
	2267390	C to G	Synpcc7942_2188	2,266,131-2,267,534, Complement	Gly49Arg
	2407863	G to T			
SU92	1746449	A to C	Synpcc7942_1677	1745500-1,746,597, Complement	Val50Gly
	2549843	C to T	Synpcc7942_2468 (*dnaK2*)	2,548,622-2,550,526, Direct	Arg408Cys
SU94	1930842	G to A	Synpcc7942_1860 (*rre1*)	1,930,475-1,931,182, Complement	Pro114Leu
SU101	2194769	T to C	5' upstream of Synpcc7942_2114 (*sasA*)	2,194,827-2,195,990, Direct	Promoter mutation?
SU102	1746449	A to C	Synpcc7942_1677	1745500-1,746,597, Complement	Val50Gly
	1930992	A to C	Synpcc7942_1860 (*rre1*)	1,930,475-1,931,182, Complement	Val64Gly
SU103	2195072 to 2195090	19 bp deletion	Synpcc7942_2114 (*sasA*)	2,194,827-2,195,990, Direct	Ser83fs
SU104	1746449	A to C	Synpcc7942_1677	1745500-1,746,597, Complement	Val50Gly
	1930613	C to T	Synpcc7942_1860 (*rre1*)	1,930,475-1,931,182, Complement	Met190Ile

Table. 1 Analysis of whole genome sequencing of suppressor mutation caused by *hik34* deletion. Genomic DNA was extracted from the *hik34* deletion mutants and Genomic DNA (600 ng) was fragmented to an average length of 500 bp to prepare the sequencing libraries. Paired-end sequencing was carried out for 300 cycles (details are described in materials and method).

2.3.3 *rre1*^{P114L} and *sasA*^{S83fs} mutations are epistatic to the phenotypes caused by the *hik34* deletion

The transcriptional activation of *hspA* under temperature upshift was examined for isolated suppressing mutants, SU92, SU94 and SU103, and compared with that for NB34. As the results, the activation alleviated in NB34 was basically restored in these strains (Fig.2.3), indicating the slow growth and the alleviated response were somehow linked event.

Mutation in the *rre1* gene occurred in SU94, SU102 and SU104 independently (mutation sites are shown in Table. 1), suggesting the involvement of identified base changes in this gene for the suppression. Among the three *rre1* mutation alleles, the *rre1* mutation in SU104 causing the 114th Pro to Leu amino acid change was chosen for further analysis as this is the unique candidate suppressor allele in this strain. Mutations in the *sasA* gene were identified in multiple strains, but a 19-bp deletion resulting in the frame shift after the 83rd Ser codon is again the unique candidate suppressor allele found in SU103. Together with a likely suppressor candidate mutation occurred in *dnaK2* resulting in the 408th Arg to Cys change in SU92, we first planned to transfer each of these three mutation alleles into the WT genome background for further genetic analysis. For this, DNA fragments in which spectinomycin resistant gene was located between the mutated gene ORF and the downstream DNA region were constructed by PCR and used to transform WT cells to introduce these mutations onto the WT genome (Figs. 2.4, 2.5 and 2.6). After transformation several single colonies were isolated and checked the transformation frequency by DNA sequencing after PCR amplification of the mutated region. Eight single colony were picked up and analyzed to confirm the transfer of *sasA*^{S83fs} mutation. *sasA*^{S83fs} mutations were successfully transferred seven clones to the WT background and named as S103. Eight single clones were also picked up and analyzed to confirm the transfer of *rre1*^{P114L} to confirm the transfer of *rre1*^{P114L} mutation. *rre1*^{P114L} mutation were successfully transformed to five clones among eight clones and named them as R94.

Both R94 and S103 showed the similar apparent growth and the heat inducible transcription of *hspA* as WT (Fig. 2.3B, 2.7B). On the other hand, we could not isolate a strain harboring the *dnaK2*^{R408C} mutation among 20 single clones. This is probably because the *dnaK2*^{R408C} mutation without the *hik34* deletion is toxic for the cell by presently unknown reason. Subsequently, we deleted the *hik34* gene of R94 and S103 and found the resultant double mutants, named RH94 and SH103, respectively, could grow as WT cells (Fig. 2.2). Thus, it was confirmed that these *rre1*^{P114L} as well as *sasA*^{S83fs} mutations could suppress the slow growing phenotype of the *hik34* deletion mutant.

Heat inducible Rre1 phosphorylation and *hspA* transcription was examined for RH94 and SH103 (Fig.2.7C, 2.7D). In the presence of *rre1*^{P114L} or *sasA*^{S83fs} mutation, defects of the *hik34* mutant for the *hspA* transcriptional activation and the Rre1 phosphorylation after temperature upshift were resumed completely by *rre1*^{P114L} and partially by *sasA*^{S83fs}. This result suggested that these mutations are epistatic to the *hik34* deletion mutation, and these gene products are likely working downstream of Hik34 during the signaling event. These genetic lines of evidence, together with previous *in vitro* results (Sato et al. 2007, Kato et al. 2012), indicated that Rre1 phosphorylation is occurring basically dependent on Hik2 where this phosphorylation event is modulated by Hik34 through the SasA and Rre1 function.

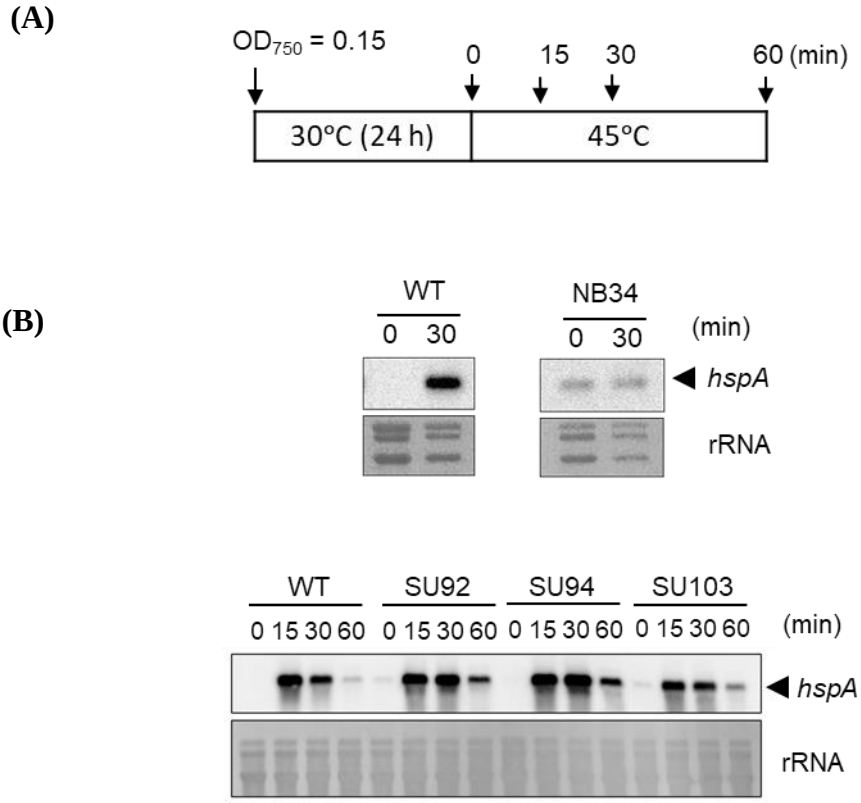

Fig. 2.3 Deletion of the *hik34* gene resulted in occurrence of suppressor mutations that negated the defects in the growth and the response to temperature upshift.

(A) Experimental scheme of temperature upshift experiments. Cells were inoculated at an initial OD_{750} of about 0.15 in BG-11 liquid medium at 30°C and incubated for 24 h. After the temperature upshift to 45°C, cells were collected at indicated times and subjected to the analyses. **(B)** Analysis of the *hspA* transcripts after temperature upshift. Cells were collected at indicated times and analyzed. Total RNAs were extracted and 3 µg RNA per lane was subjected to northern blot analysis. The *hspA* transcripts were detected using DIG-labelled *hspA* probe. rRNA was the loading control. The split northern hybridization data of WT and NB34 was derived from the identical membrane.

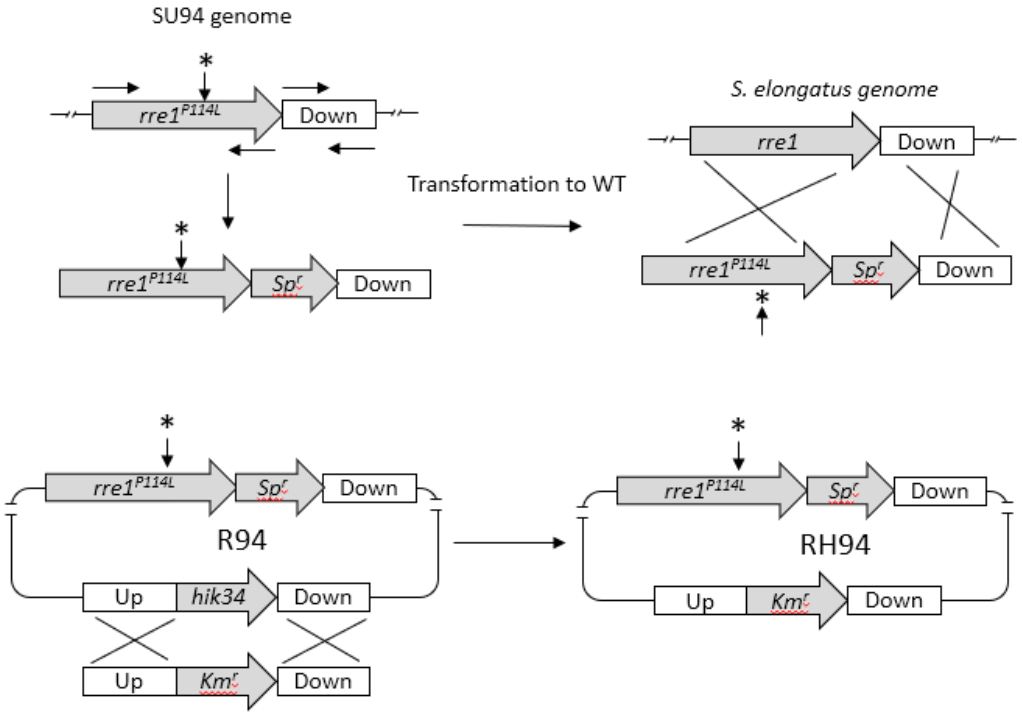

Fig. 2.4. Genetic analysis of *rre1*^{P114L} mutation.

The rre1^{P114L} ORF and the 3'-downstream DNA sequence were amplified from SU94 by PCR using DNA primer sets [rre1-Fw-NotI and rre1-Rv-BamHI] and [rre1DN-Fw-XhoI and rre1DN-RV-KpnI], respectively. These fragments were inserted into both side of the spectinomycin resistance gene of pBΩH (Hasegawa et al. 2020) by standard procedures using restriction enzyme digestion and ligation. The resultant plasmid was transformed to WT for the spectinomycin resistance, and rre1^{P114L} containing transformants were screened by direct genome sequencing to obtain R94. Subsequently, the *hik34::Km* DNA cassette were transformed to obtain RH94. The primers were listed in Table. S2.

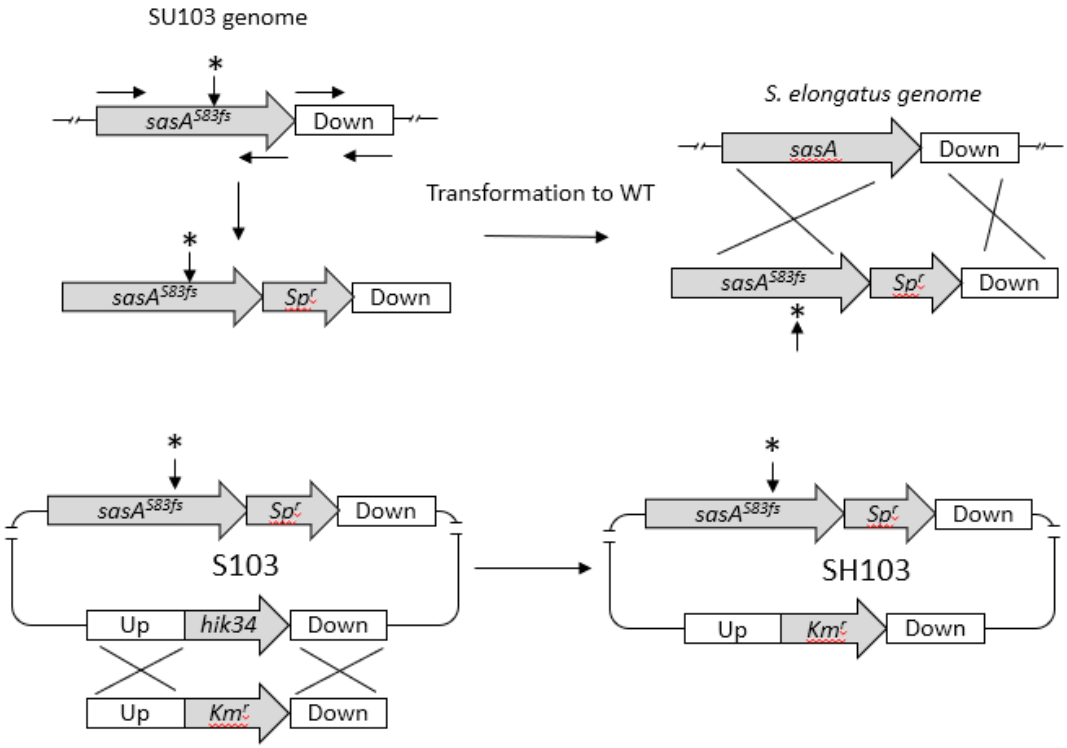

Fig. 2.5 Genetic analysis of *sasA*^{S83fs} mutation.

The *sasA*^{S83fs} ORF and the 3'-downstream DNA sequence were amplified from SU103 by PCR using DNA primer sets [sasAUp-F-SacI and sasA-Rv-NotI] and [sasADN-FW-XhoI and sasADN-RV-KpnI], respectively. These fragments were inserted into both side of the spectinomycin resistance gene of pBΩH by standard procedures using restriction enzyme digestion and ligation. The resultant plasmid was transformed to WT for the spectinomycin resistance, and *sasA*^{S83fs} containing transformants were screened by direct genome sequencing to obtain S103. Subsequently, the *hik34::Km* DNA cassette were transformed to obtain SH103. The primers were listed in Table. S2.

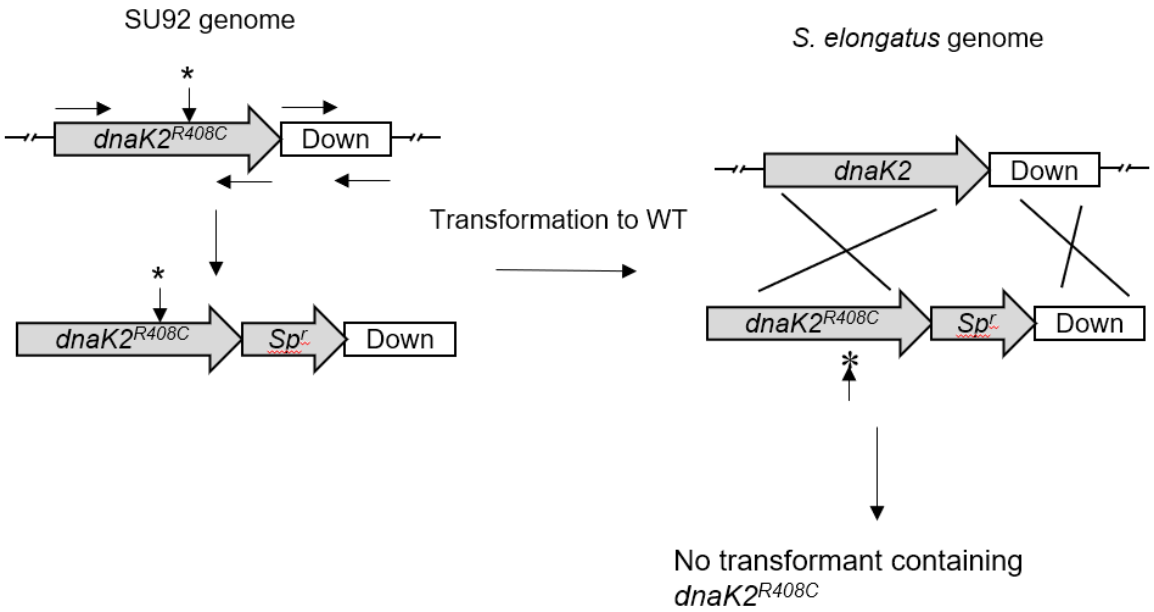

Fig. 2.6 *Genetic analysis of dnaK2^{R408C}* mutation.

The *dnaK2^{R408C}*ORF and the 3'-downstream DNA sequence were amplified from SU92 by PCR using DNA primer sets [dnaK2-Fw-SacI and dnaK2-Rv-BamHI-SmaI] and [2469-Fw-SalI and 2469-Rv-KpnI], respectively. These fragments were inserted into both side of the spectinomycin resistance gene of pBΩH by standard procedures using restriction enzyme digestion and ligation. The resultant plasmid was transformed to WT for the spectinomycin resistance, and *dnaK2^{R408C}*containing transformants were screened by direct genome sequencing. However, no transformant containing *dnaK2^{R408C}* was obtained. The primers were listed in Table. S2.

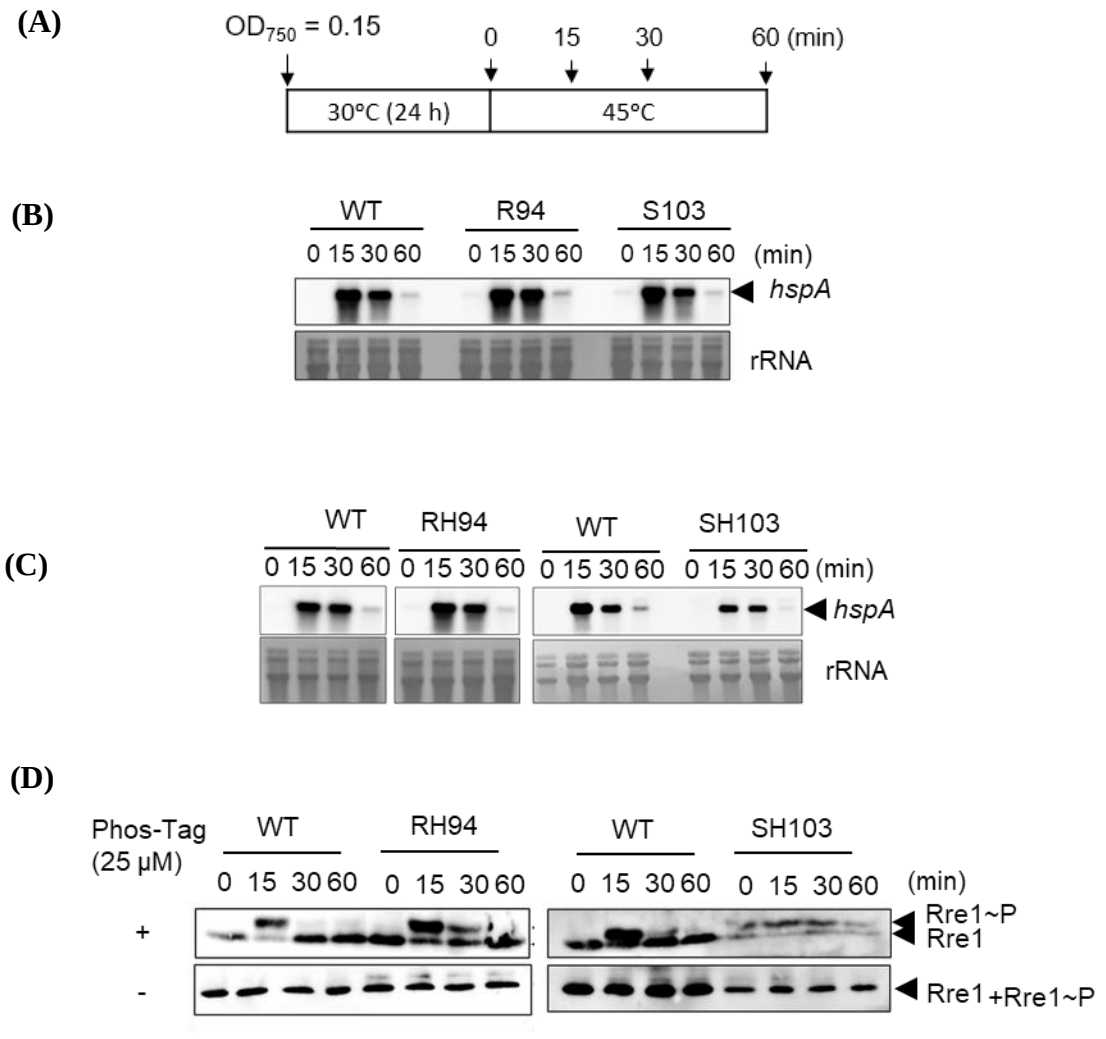

Fig. 2.7 Heat shock response in genetically defined suppressor mutants.

(A) Experimental scheme of temperature upshift experiments. Cells were inoculated at an initial OD_{750} of about 0.15 in BG-11 liquid medium at 30°C and incubated for 24 h. After the temperature upshift to 45°C, cells were collected at indicated times and subjected to the analyses. Analysis of the *hspA* transcripts after temperature upshift. Cells were collected at indicated times and analyzed. Total RNAs were extracted and 3 μg RNA per lane was subjected to northern blot analysis. The *hspA* transcripts were detected using DIG-labelled *hspA* probe.

rRNA was the loading control. **(B, C)** Analysis of the *hspA* transcripts during the temperature upshift in genetically defined *rre1* and *sasA* mutants. Cells were collected at indicated times and analyzed. Total RNAs were extracted and 3 µg RNA per lane was subjected to northern blot analysis. The *hspA* transcripts were detected using DIG-labelled *hspA* probe. rRNA was the loading control. The split northern hybridization data of WT and RH94 was derived from the identical membrane **(D)** The Rre1 protein level and phosphorylation status during the temperature upshift in genetically defined *rre1* and *sasA* mutants. Cells were collected at indicated times after temperature upshift and proteins were extracted. 20 mg of proteins were separated by Phos-tag SDS-PAGE and Rre1 proteins were detected by using custom made rabbit-anti-Rre1 antibody. The phosphorylated and unphosphorylated Rre1 bands are indicated by arrowheads.

2.4 Summary of Chapter 2

Hik2, Hik34 and Rre1 are conserved modulator of Cyanobacterial two component system. Functional properties of Rre1 are well established compared with the Hik2 and Hik34, still there are many questions unsolved regarding the activation mechanism. Previous study revealed Hik34 is a positive regulator for heat inducible Rre1 phosphorylation and downstream genes transcription (Kobayashi et al. 2017). In this chapter, suppressor mutations were identified in *hik34* deletion mutant and heat inducible transcriptional and phosphorylation properties were independent of Hik34. Restarting of alleviated heat inducible induction in suppressor mutant, we revised a model of heat inducible two component system composed of Hik2-Rre1. The interaction and phosphor-transfer between Hik2 and Rre1 is well established in previous study (Sato et al. 2007, Kato et al. 2012) whereas *hik34* less mutant in *Synechocystis* showed heat induced transcriptional activation under heat (Suzuki et a. 2006), that concludes Hik2-Rre1 is a cognate two-component system for the heat inducible induction. Moreover furthermore, acquisition of suppressor mutation to stabilize the *hik34* deletion mutant suggested that Hik34 could be involved in repressing an unknown antagonizing factor that alleviates heat inducible induction. Further analysis is required to characterize the involvement of suppressor mutation in heat inducible induction.

Chapter 3

Hik2, a conserved histidine kinase activates under reduced state of Plastoquinone pool, and an oxidation event represses Hik2-Rre1 module

3.1 Introduction

Hik2 is a highly conserved histidine kinase among cyanobacteria. Orthologous proteins were also found from plant chloroplasts (Puthiyaveetil and Allen 2009), which are known as chloroplast sensory kinase (CSK), and the conserved GAF domain among them has been suggested to involve its sensory function (Ashby and Houmard 2006). Recent biochemical analysis revealed that Hik2 of *Synechocystis* is an iron-sulfur protein containing a highly redox responsive [3Fe-4S] (Ibrahim et al. 2020). The *Synechocystis* Hik2 protein contains a GAF domain likely sensing environmental changes, and a conserved cysteine residue near the N-terminus of the GAF domain was involved in the assembly of the Fe-S cluster. It was proposed that Hik2 is activated under PQ oxidizing conditions which is mediated by [3Fe-4S] cluster attached with the conserved GAF domain (Ibrahim et al. 2020). Meanwhile, comparison of Hik2 proteins predicted from sequenced genome sequences found that some Hik2 proteins, including of *S. elongatus*, lacks the conserved cysteine residue in their GAF domain (Ibrahim et al. 2020). Lines of evidence for the Hik2-Rre1 TCS module have been obtained. Firstly, Hik2-Rre1 specific interaction was shown in a yeast two-hybrid assay in *S. elongatus* (Sato et al. 2007, Kato et al. 2012). Secondly, *in vitro* phosphor-transfer analysis revealed that Hik2 could phosphorylate Rre1 using *S. elongatus* and *Synechocystis* proteins (Kato et al. 2012, Vidal et al. 2015, Ibrahim et al. 2016). In this study, conservation of cysteine residue in GAF domain of Hik2s are shown as well as PQ pool redox dependent regulation of Hik2-Rre1 pathway was shown.

3.2 Materials and methods.

3.2.1 *Bacterial strains, culture media and mutant strain constructions*

S. elongatus (WT) and its mutants were grown in BG-11 (Rippka 1988) liquid medium (2% CO_2 aeration) or BG-11 solid medium containing 1.5% w/v agar at 30°C under continuous fluorescent light (30 µmol photons/m^2/s). BG-11 medium. Cultures were grown to OD_{750}=0.5 in BG-11 liquid medium for to examine in several condition. Temperature upshift experiments were performed by transfer the culture media to water bath (45°C) placed in the same incubation condition mentioned above. Photosynthesis inhibitor, DCMU and DBMIB (Sigma-aldrich, St. Louis, Missouri, United States) were used at a concentration of 10 µM. DCBQ (Wako chemicals, Tokyo, Japan) were used at a concentration of 100 µM with 5 mM or without reductant DTT (Nacalai Tesque, Inc., Kyoto, Japan).

3.2.2 Multiple sequence alignment of GAF domain of Hik2 homologs

A multiple sequence alignment of GAF domain of Hik2 were prepared using the homologs of Hik2, and the N-terminal conserved portion was shown. Classification of freshwater cyanobacteria, marine cyanobacteria and chloroplast CSK are also indicated. Conserved cysteine residues were marked as red arrowhead. Amino acid sequence of GAF domain of Hik2 homologs were retrieve from the databases, Cyanobase (http://genome.microbedb.jp/cyanobase/) (Nakamura et al. 1998), KEGG (https://www.kegg.jp/) (Kanehisa et al. 2016) or NCBI (https://www.ncbi.nlm.nih.gov/) (Pruitt et al. 2007) , as *S. elongatus* (Synpcc7942_0453), *Synechocystis* sp. PCC 6803 (Slr1147), *Nostoc punctiforme* PCC 73102 (Npun_R4028), *Microcystis aeruginosa* NIES-88 (MAN88_15620), *Synechococcus* sp. PCC 7002 (SYNPCC7002_A1954), *Thermosynechococcus elongatus* BP-1 (tlr0195), *Prochlorococcus marinus* MIT 9301 (P9301_02921), *Prochlorococcus marinus* MIT 9202 (P9202_RS05345), *Prochlorococcus*

marinus MED4 (PMM0269), *Synechococcus* sp. RS9916 (RS9916_39061), *Synechococcus* sp. CC9605 (Syncc9605_0240), *Synechococcus* sp. WH 5701 (WH5701_01535), *Cyanidioschyzon merolae* (CYME_CMP021C), *Arabidopsis thaliana* (At1g67840), and *Phaeodactylum tricornutum* (PHATRDRAFT_41268). Full length amino acid sequence of Hik2 homologs were used to determine the GAF domain using SMART (Schultz et al. 2000) (http://smart.embl-heidelberg.de/). Multiple sequence alignment was performed using ClustalW (Thompson et al. 1994) (https://clustalw.ddbj.nig.ac.jp/) (pairwise alignment criteria: Gap opening penalty: 10.00, Gap extension penalty: 2.00; Multiple alignment criteria: Gap opening penalty: 10.00; Gap extension penalty: 2.00). Conserved cysteine residue was marked as red filled box and indicated with a red open arrowhead. Other conserved amino acids are marked as blue filled box.

3.2.3 ***RNA analysis***

Cells were harvested from the culture tubes after each experimental time point and collected using centrifugation (7000 × g, 2 m, 4^{o}C) and stored at -80^{o}C for further analysis. Total RNA was extracted from the *S. elongatus* cells using hot phenol method (Mironov, K.S., Los, D.A. 2015) and 3 µg of total RNA were used for the northern hybridization analysis (Seki et al. 2007). For *hspA* probe preparation, the following primers were used to amply the *hspA* DNA fragment: hspA-Prb-Fw and hspA-Prb-Rw. DIG dNTPs (DIG DNA labelling mix, Roche, Basel, Switzerland) were labelled with the DNA by PCR reaction. The primers used for the probe amplification were listed in Table. S2.

3.2.4 ***Immunoblot and Phos-tag SDS-PAGE analyses***

Details method of Phos-Tag SDS-PAGE is described at the supplemental section.

3.3 Results

3.3.1 *S. elongatus Hik2 shares the conserved GAF domain*

Hik2 is a highly conserved histidine kinase among cyanobacteria. Orthologous proteins were also found from plant chloroplasts (Puthiyaveetil and Allen 2009), which are known as chloroplast sensory kinase (CSK), and the conserved GAF domain among them has been suggested to involve its sensory function (Ashby and Houmard 2006). In a previous study, a specific Cys residue found near the GAF domain N-terminus was shown to bind to [3Fe-4S] cluster in *Synechocystis* and two CSKs (*Arabidopsis thaliana* and *Phaeodactylum tricornutum*), which is critical for sensing PQ redox status (Ibrahim et al. 2020). While this Cys residue is conserved among divergent cyanobacterial Hik2, it was also suggested that the Cys residue is not found in the Hik2 GAF domain in *S. elongatus*, contradicting with the annotated Hik2 sequence obtained from two genome databases (https://www.genome.jp/entry/syf:Synpcc7942_0453; http://genome.microbedb.jp/cyanobase/GCA_000012525.1/genes/Synpcc7942_0453). To ascertain this discrepancy, we examined the whole genome sequencing results of our *S. elongatus* strains in detail and found the conservation of the Cys residue (Fig. 3.1 and 3.2). Thus, the GAF domain structure is conserved in *S. elongatus* as well, and the conserved Cys residue is likely involved in Fe-S cluster assembly and responsible for sensing the PQ redox status.

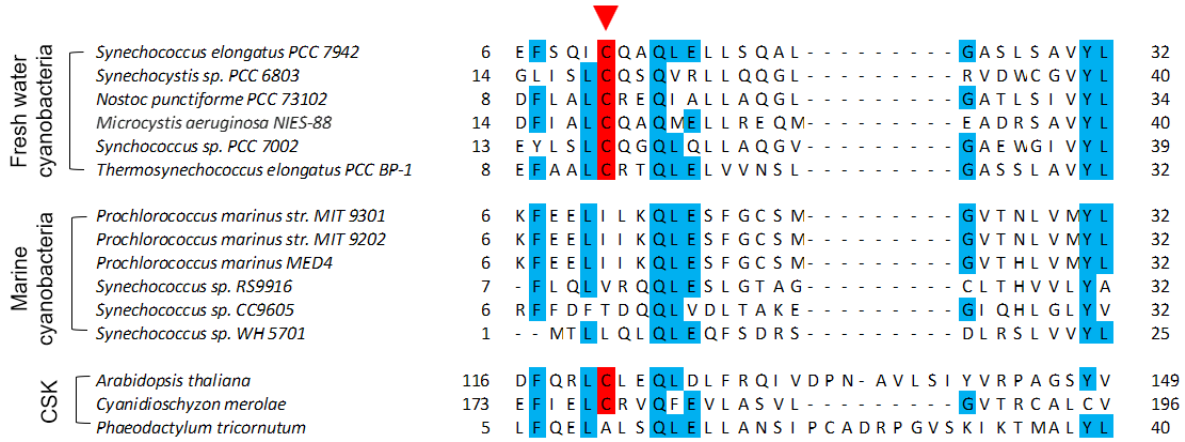

Fig. 3.1 Conservation of the specific Cys residue among the GAF domain of Hik2 homologs and CSKs

A multiple sequence alignment of GAF domain of Hik2 were prepared using the homologs of Hik2, and the N-terminal conserved portion was shown. Classification of freshwater cyanobacteria, marine cyanobacteria and chloroplast CSK are also indicated. Conserved cysteine residue was marked as red filled box and indicated with a red open arrowhead. Other conserved amino acids are marked as blue filled box.

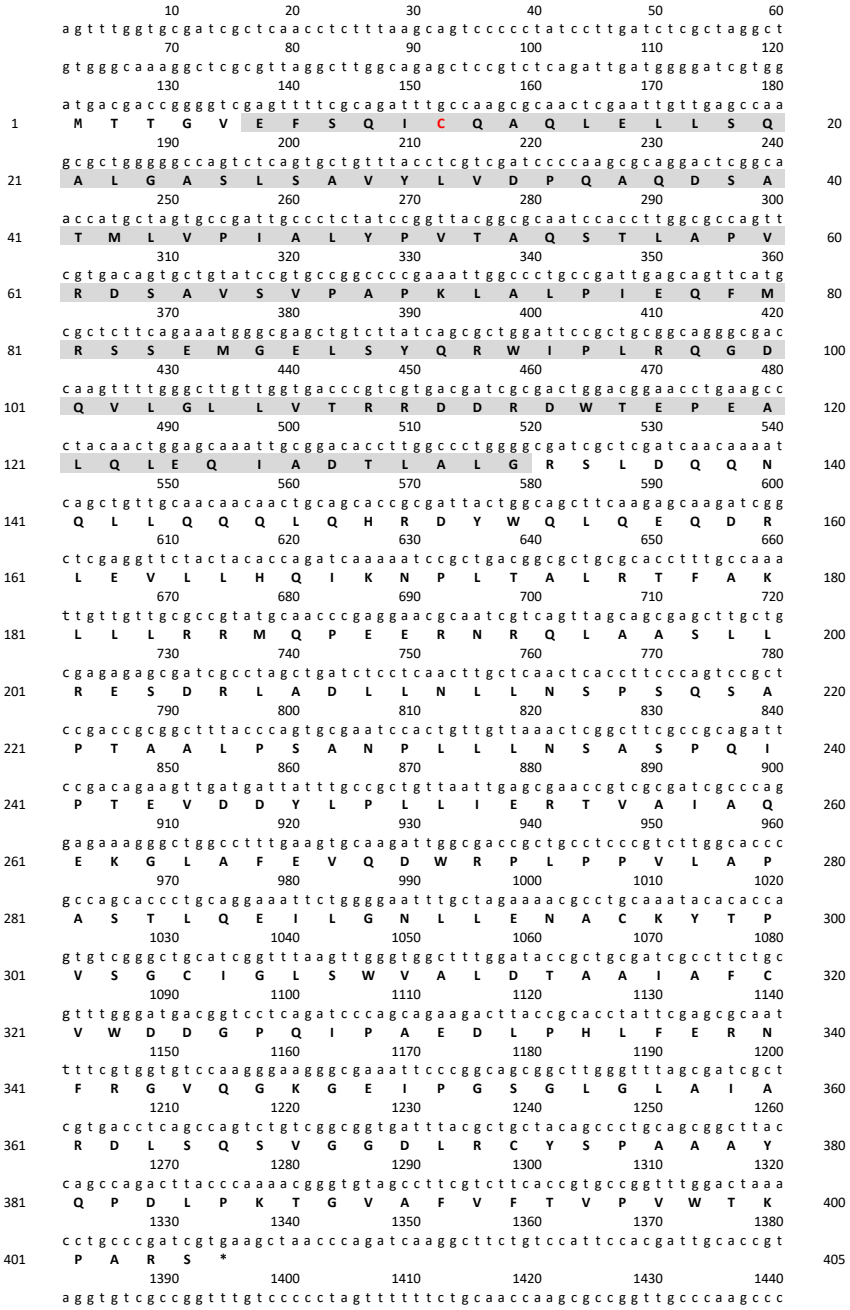

Fig. 3.2 Structure of the *hik2* gene in *S. elongatus*.

The nucleotide sequence and the deduced amino acid sequence of Hik2 are shown. The translated stop codon is marked by an asterisk. The gray marked is denoted as the conserved GAF domain and the conserved Cys residue is marked with red letter.

3.3.2 Reduced state of PQ activates Rre1 phosphorylation

Giving the conserved Hik2 GAF domain, we considered that the Hik2-Rre1 signaling event is likely modulated by the proposed upstream PQ redox status in *S. elongatus* (Ibrahim et al. 2020). To examine this, changes of Rre1 phosphorylation status were monitored after the addition of photosynthetic electron transfer inhibitors, 3-(3,4-dichlorophenyl)-1,1-dimethylurea) (DCMU) or 2,5-dibromo-6-isopropyl-3-methyl-1,4-benzoquinone (DBMIB) to the culture medium, which is expected to oxidize or reduce the PQ pool of the photosynthetic electron transport chain, respectively. As the results, DBMIB but not DCMU rapidly induced the Rre1 phosphorylation, suggesting that the reduced PQ pool activated the Hik2 dependent Rre1 phosphorylation (Fig. 3.3C). The *hspA* transcription that is under the control of phosphorylated Rre1 was consistently activated in accordance with the Rre1 phosphorylation. Interestingly, we found the *hspA* transcription was also activated by the addition of DCMU without Rre1 phosphorylation (Fig. 3.3B). This indicated the presence of the *hspA* transcription activation pathway independent of the Rre1 phosphorylation, but it is unclear whether this activation is also dependent on or independent of unphosphorylated Rre1.

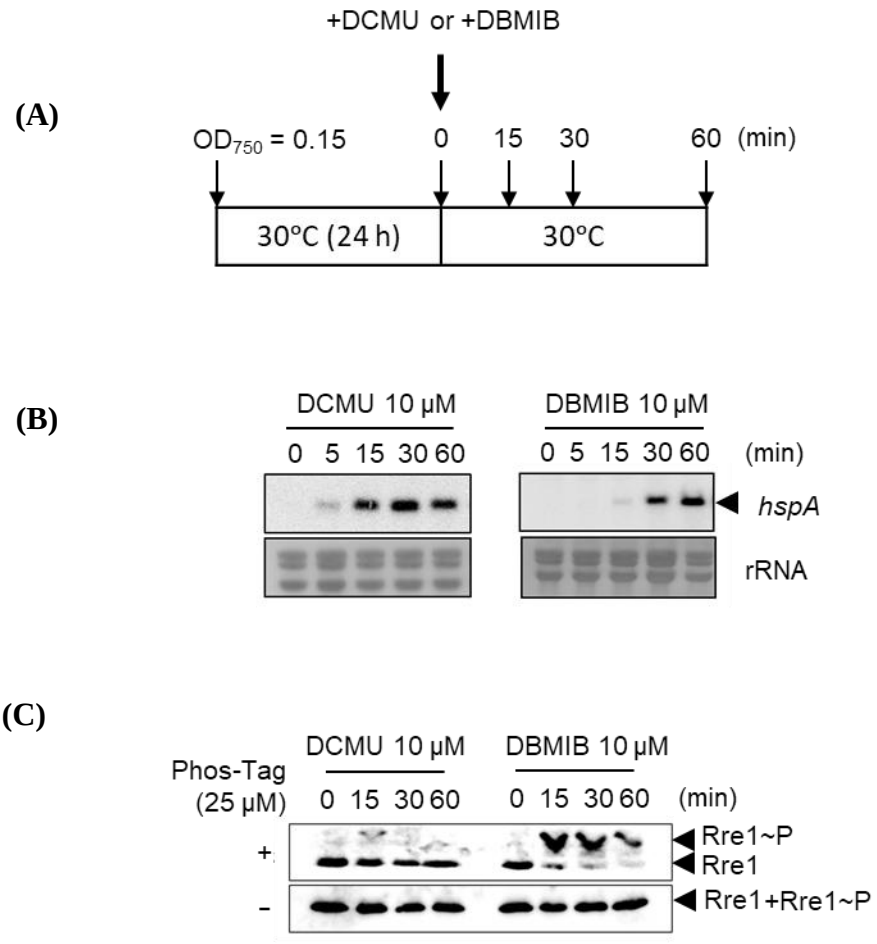

Fig. 3.3 Activation of Hik2-Rre1 module in the presence of photosynthetic electron transport inhibitors

(A) Experimental scheme. The WT cells were inoculated at an initial OD_{750} of about 0.15 in BG-11 liquid medium and incubated 24 h. DCMU (10 µM) and DBMIB (10 µM) were added to the culture media, and cells were collected at indicated times. **(B)** Analysis of the *hspA* transcripts after addition of DCMU (10 µM) or DBMIB (10 µM). Cells were harvested at indicated times and analyzed. Total RNAs were extracted and 3 µg RNA per lane was subjected to northern blot analysis. The *hspA* transcripts were detected using DIG-labelled *hspA* probe. rRNA was the loading control. **(C)** Effect of DCMU/DBMIB on the Rre1 protein level and the phosphorylation status. DCMU (10 µM) or DBMIB (10 µM) were added to culture media. Samples were collected as in **(B)** and immunoblot, and phos-tag PAGE analyses were performed to examine the Rre1 protein accumulation and the phosphorylation status. The phosphorylated and unphosphorylated Rre1 bands are indicated by arrowheads.

3.3.3 Changes of cellular redox status dominantly affected heat inducible Rre1 phosphorylation.

Rre1 phosphorylation that was considered occurring dependent on Hik2 was enhanced under temperature upshift as well as under PQ reducing condition. To further understand the interrelationship between the two responses, we examined for the effect of cellular redox change induced by 2,6-dichloro-1,4-benzoquinone (DCBQ), which was previously showed to oxidize PQ pool by accepting electrons from PSII (Kashino et al. 1996, Schuurmans et al. 2014), on the heat dependent Rre1 phosphorylation and the resultant *hspA* gene transcriptional activation. As the result, the heat inducible responses were clearly disappeared when DCBQ was added to the medium prior to the temperature upshift (Fig. 3.4B and 3.4C). To confirm whether the DCBQ effect was occurring through some reduction event as expected, DCBQ was reduced with dithiothreitol (DTT) before the use and examined for the effect on the heat inducible response. As the result, reduced DCBQ lost the effect on the response, and thus oxidizing power of DCBQ was shown to be required to diminish the heat shock response (Fig. 3.4D). Meanwhile, the responsible DCBQ oxidized target remains to be examined.

(A)

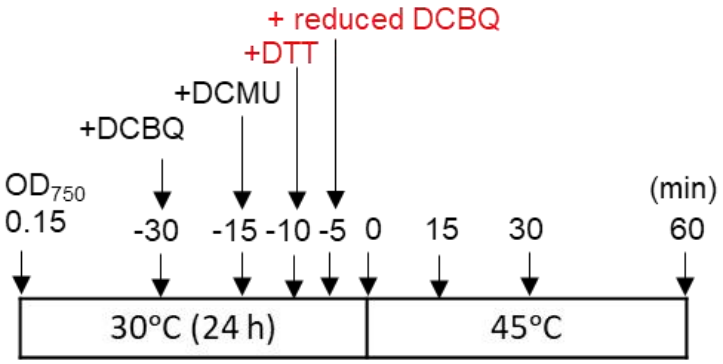
+ reduced DCBQ
+DTT
+DCMU
+DCBQ
OD750
0.15
-30
-15
-10
-5
0
15
30
(min)
60
30°C (24 h)
45°C

(B)

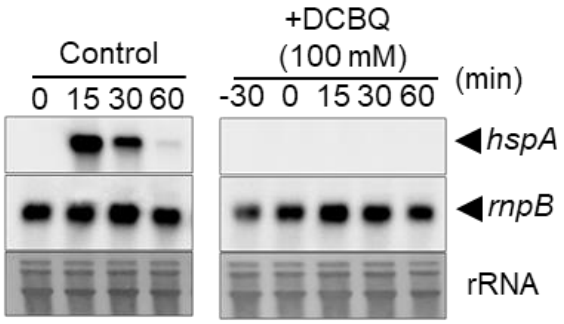
Control
+DCBQ
(100 mM)
0 15 30 60
-30 0 15 30 60
(min)
hspA
rnpB
rRNA

(C)

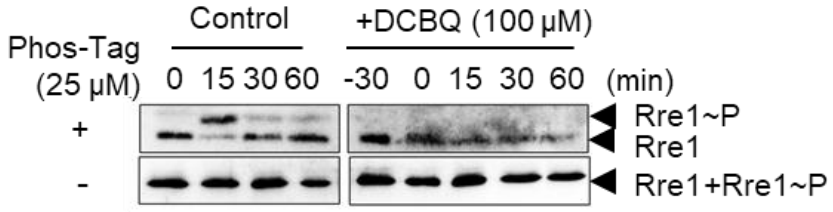
Control
+DCBQ (100 µM)
Phos-Tag
(25 µM)
0 15 30 60
-30 0 15 30 60
(min)
+
-
Rre1~P
Rre1
Rre1+Rre1~P

(D)

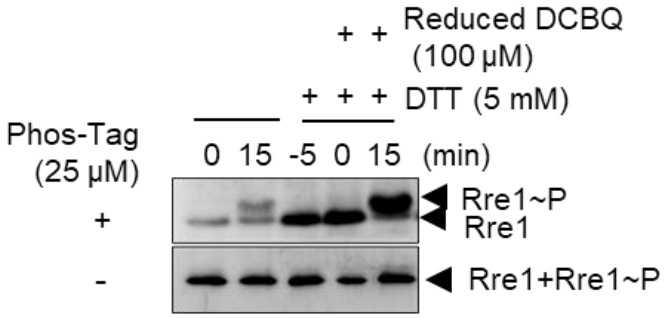
+ +
Reduced DCBQ
(100 µM)
+ + + DTT (5 mM)
Phos-Tag
(25 µM)
0 15 -5 0 15 (min)
+
-
Rre1~P
Rre1
Rre1+Rre1~P

Fig. 3.4 Effect of DCBQ treatment in Hik2-Rre1 module under high temperature

(A) Experimental scheme. The WT cells were inoculated at an initial OD_{750} of about 0.15 in BG-11 liquid medium and incubated 24 h. Cells were collected periodically before and after temperature upshift in the presence of DCBQ, DTT and/or reduced DCBQ. **(B)** Analysis of the *hspA* transcripts after temperature upshift in the presence of DCBQ (100 µM). DCBQ was added to culture media 30 m before temperature upshift. Cells were collected at indicated times and subjected to the analysis. rRNA was the loading control. The split northern hybridization data of control and DCBQ addition was derived from the identical membrane. **(C)** Analysis of the Rre1 phosphorylation after temperature upshift in the presence of DCBQ. DCBQ (100 µM) was added as in **(B),** and cells were collected at indicated times. Proteins were separated by Phos-tag SDS-PAGE and Rre1 proteins were detected by using custom made rabbit-anti-Rre1 antibody. The phosphorylated and unphosphorylated Rre1are indicated by arrowheads. **(D)** Analysis of the Rre1 phosphorylation after temperature upshift in the presence of pre-reduced DCBQ. DTT (5 mM) and DCBQ (100 µM) were incubated on ice for 5 m under dark to prepare pre-reduced DCBQ. DTT (5 mM) was firstly added to the medium at -10 m to estimate the effect of DTT, and then the pre-reduced DCBQ (100 µM) was added to the medium. Cells were harvested at -5, 0 and 15 m for the analysis. Left and right lanes are controls for without drugs and only DCBQ (100 µM), respectively. Proteins were separated by Phos-tag SDS-PAGE and Rre1 proteins were detected by using custom made rabbit-anti-Rre1 antibody. The phosphorylated and unphosphorylated Rre1 bands are indicated by filled and open arrowheads, respectively.

3.4 Summary of Chapter 3

In this chapter, regulatory signal of Hik2 activation is shown. Hik2 is orthologous to CSK (Chloroplast sensor kinase) from higher lineages, which was proposed to sense redox state of the plastoquinone pool (Puthiyaveetil and Allen, 2009). Recent study revealed Hik2 is a redox responsive Fe-S protein and possess a redox responsive [3Fe-4S] cluster in cyanobacteria as well as in chloroplast (Ibrahim et al. 2020). Typically, Fe ion in Fe-S cluster is typically bound by cysteine that is the redox sensor of Fe-S cluster. CSK, as well as Hik2 has a conserved cysteine residue in its GAF domain near N-terminal region that possibly related to redox sensing. GAF domain may be involved in binding with PQ pool that increase the possibility that Hik2 is sensing the redox signal near the PQ pool. As Hik2 is PQ pool redox sensing histidine kinase, our findings suggested that reduced PQ pool induced the Hik2 activity by phosphorylating Rre1. Whereas oxidized PQ pool unlikely phosphorylate Rre1 that suggested Hik2 could sense reduced state of PQ pool, but not oxidized state. Though, Rre1 phosphorylation was absent in oxidized PQ pool, *hspA* transcription was appeared which indicating that there is a separate pathway of *hspA* induction independent of Rre1 phosphorylation. Moreover, an unknown oxidation event by DCBQ completely diminished both heat inducible Rre1 phosphorylation and *hspA* transcription. Whereas reduced DCBQ lost its oxidizing power which couldn't diminish heat inducible Rre1 phosphorylation that suggests the cellular redox state is dominantly affect heat inducible Rre1 phosphorylation.

Chapter 4

Quenching of the heat induced Hik2-Rre1 response, and Relationship between the Hik2-Rre1 response and the PQ redox state

4.1 Introduction

In previous chapters, it was shown that heat inducible Rre1 phosphorylation and downstream gene transcription was declined after relatively short period (<15). The declination of the heat shock response in *Escherichia coli* was previously well known and a negative feedback loop is involved in repressing the activation. a major chaperone protein DnaK is involved in the repression of the heat shock transcriptional activation, where DnaK interacts with the heat shock sigma factor 32 and results in the rapid degradation (Gamer et al. 1996). Heat induced Rre1 phosphorylation can activate many downstream chaperone genes including DnaK2, GroEL, HtpG, HspA etc. In cyanobacteria, there is a possibility that heat inducible chaperone genes products could regulate the repression the heat inducible transcription. In this study, the effect of translation inhibitor under heat shock was observed to determine the role of heat inducible chaperone gene products in repression of the response. In previous chapter, it was shown that Hik2-Rre1 TCS module is activated under reduced state of PQ pool and a unknown oxidation event is repressing the Hik2-Rre1 TCS module. The relationship between PQ redox state and heat shock response is still unknown. In this study, the relationship Hik2-Rre1 related response and PQ redox state were shown.

4.2 Materials and Method

4.2.1 Bacterial strains, culture media and mutant strain constructions

S. elongatus (WT) and its mutants were grown in BG-11 (Rippka 1988) liquid medium (2% CO_2 aeration) or BG-11 solid medium containing 1.5% w/v agar at 30ºC under continuous fluorescent light (30 µmol photons/m^2/s). Cultures were grown to OD_{750}=0.5 in BG-11 liquid medium for to examine in several condition. Temperature upshift experiments were performed by transfer the culture media to water bath (45˚C) placed in the same incubation condition mentioned above.

4.2.2 RNA analysis

Cells were harvested from the culture tubes after each experimental time point and collected using centrifugation (7000 × g, 2 m, 4ºC) and stored at -80ºC for further analysis. Total RNA was extracted from the *S. elongatus* cells using hot phenol method (Mironov, K.S., Los, D.A. 2015) and 3 µg of total RNA were used for the northern hybridization analysis (Seki et al. 2007). For *hspA* probe preparation, the following primers were used to amply the *hspA* DNA fragment: hspA-Prb-Fw and hspA-Prb-Rw. DIG dNTPs (DIG DNA labelling mix, Roche, Basel, Switzerland) were labelled with the DNA by PCR reaction. The primers used for the probe amplification were listed in Table. S2.

4.2.3 Immunoblot and Phos-tag SDS-PAGE analyses

Details method of Phos-Tag SDS-PAGE is described at the supplemental section.

4.2.4 Measurement of Redox state of PQ pool

The intracellular redox state of PQ was determined as described previously (Khorobrykh et al. 2020). *S. elongatus* cells harvested by vacuum filtration through a glass fibre filter were ground in 2 mL ice-cold ethyl acetate. The extract was transferred to a

microtube using a syringe filter, and then the liquid was removed by evaporation under vacuum. The dried sample was dissolved in 200 µL methanol, and then 90 µL-aliquots were transferred to two HPLC vials. One aliquot was analysed by HPLC without further treatment to estimate the in vivo amount of plastoquinol (reduced form of plastoquinone, PQH2). For the other aliquot, NaBH4 was added before HPLC analysis to reduce PQ to PQH2, which allowed us to estimate the total amount of PQ in the sample. The samples were analysed by HPLC using Shimadzu (Kyoto, Japan) Prominence series devices (LC-20AD, SIL-20A, CTO-20A), and a C18 reversed phase column (250 x 4.6 mm, 5 µm, InertSustain C18, GL science, Tokyo, Japan). The isocratic solvent system (methanol/ethanol, 50/50, vol/vol) had a flow rate of 1.0 ml/min, and the temperature of the column was set to 35°C. Absorption at 255 nm and fluorescence at 330 nm with excitation at 290 nm were monitored by SPD-20A and RF-20Axs instruments (Shimadzu, Kyoto, Japan), respectively. We detected PQH2 as the fluorescence peak at the retention time of 8.1 min. The peak area of PQH2 was normalised to that of chlorophyll a (absorption peak at 6.6 min retention time). The redox state of PQ was calculated as the ratio of the normalised PQH2 peak area between samples with and without NaBH4.

4.3 Results

4.3.1 Quenching of the heat induced Hik2-Rre1 response requires de *novo* protein synthesis.

During the Rre1 phosphorylation and the *hspA* transcriptional activation by temperature upshift, we noticed the response was repressed after reaching to the peak (Figs. 2.3B and 2.7D). These characteristics are different from the redox dependent response, where the once activated response continued long after that. These observations suggested the presence of specific repressing mechanism induced by heat induction. To examine whether the repression requires newly synthesized protein after the temperature upshift, the heat induction was observed in the presence of protein synthesis inhibitors as chloramphenicol and kanamycin (Fig. 4.1B, 4.1C). The results clearly indicated the repression requires *de novo* protein synthesis whereas the initial activation is not affected (Fig. 4.2).

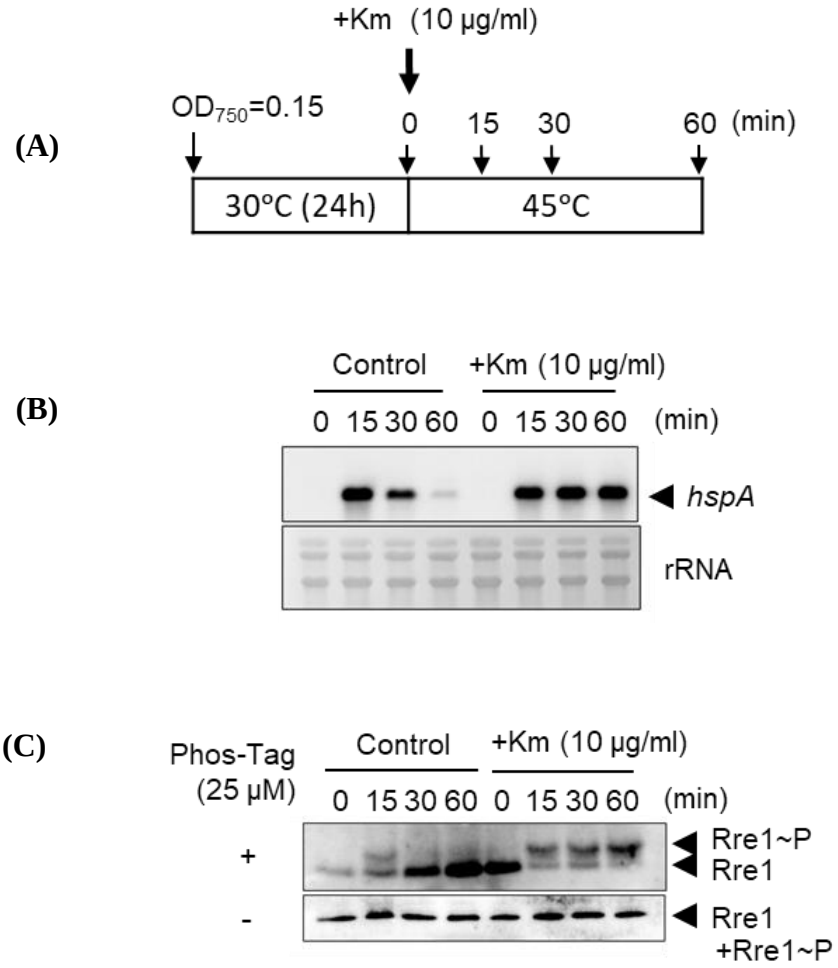

Fig. 4.1 Effect to protein synthesis inhibitor under high temperature for Hik2-Rre1 module

(A) Experimental scheme. Cells were inoculated at an initial OD_{750} of about 0.15 in BG-11 liquid medium and incubated for 24 h. At the temperature upshift to 45°C, kanamycin (10 µg/ml) was added to the medium and cells were collected at indicated times for the analyses. **(B)** Analysis of the *hspA* transcripts during the temperature upshift in the presence of kanamycin. Cells were collected at indicated times and analyzed. Total RNAs were extracted and 3 µg RNA per lane was subjected to northern blot analysis. *hspA* transcripts were detected using *hspA* probe. rRNA was the loading control. **(C)** The Rre1 protein level and phosphorylation status during the temperature upshift in the presence of kanamycin (10 µg/ml).

Cells were collected at indicated times and analyzed. Protein sample (20 mg) was separated by Phos-tag SDS-PAGE and Rre1 proteins were detected by using custom made rabbit-anti-Rre1 antibody. The phosphorylated and unphosphorylated Rre1 bands are indicated by filled and open arrowheads, respectively.

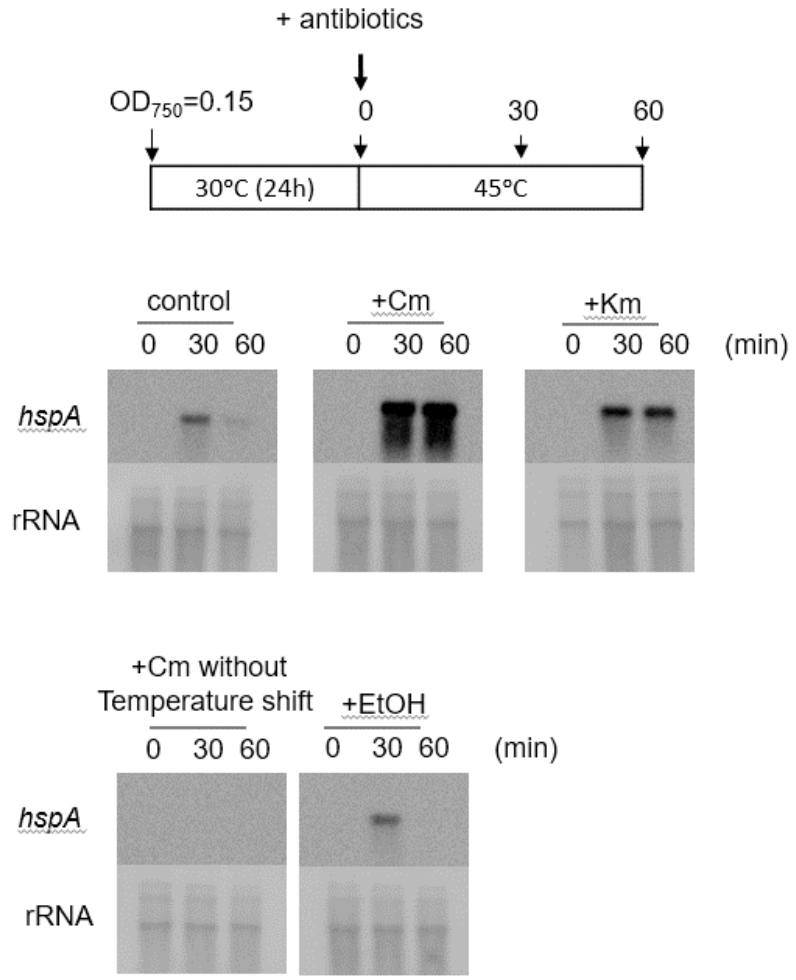

Fig. 4.2. Effect of antibiotics under temperature upshift.

Cultures of *S. elongatus* were subjected to temperature upshift (45°C) in the presence of chloramphenicol (Cm: 100 µg/ml) or kanamycin (Km: 10 µg/ml). After addition of antibiotics, cells were harvested after 0, 30, 60 m after the temperature upshift. Effects of addition of the equal amount of ethanol (solvent for chloramphenicol) and addition of chloramphenicol addition without temperature upshift were also examined as the controls. Total RNAs were extracted, and 2 µg RNA samples were subjected to northern blot analysis. *hspA* transcripts were detected using the *hspA* probe. rRNA staining was the loading control

4.3.2 Relationship between the Hik2-Rre1 response and the PQ redox state

Results obtained in this study revealed that the Hik2-Rre1 response monitored by Rre1 phosphorylation was responsive to cellular redox status as well as to temperature upshift. For the former response, Hik2 is likely sensing the status of PQ redox pool as suggested previously (Ibrahim et al. 2020) and found in this study (Fig. 3.1C). Here, we wondered the high temperature response might be indirectly induced by heat induced changes of PQ redox status. To examine this, we periodically extracted PQ from the cells during temperature upshift treatment and monitored the PQ pool redox status changes by HPLC analysis as described (1). As shown in Fig. 4.4, the PQ redox status was gradually reduced during the measurements irrespective of the temperature upshift. This is presumably because of unexpected physiological changes during our temperature upshift procedure. Thus, here was no evidence for correlation between Rre1 phosphorylation and temperature upshift. In addition, we found that the PQ pool redox status is rather oxidized by addition of kanamycin irrespective of the temperature shift, while the redox-induced Rre1 phosphorylation occurred under PQ reducing condition (Fig. 3.3C). Giving that the kanamycin treatment did not affect the onset of the heat shock response and inhibited the subsequent repression, here is again no correlation between the PQ pool redox status and the heat inducible signaling event. These results suggested that the PQ redox status and the heat shock response are regulated independently but interacting each other.

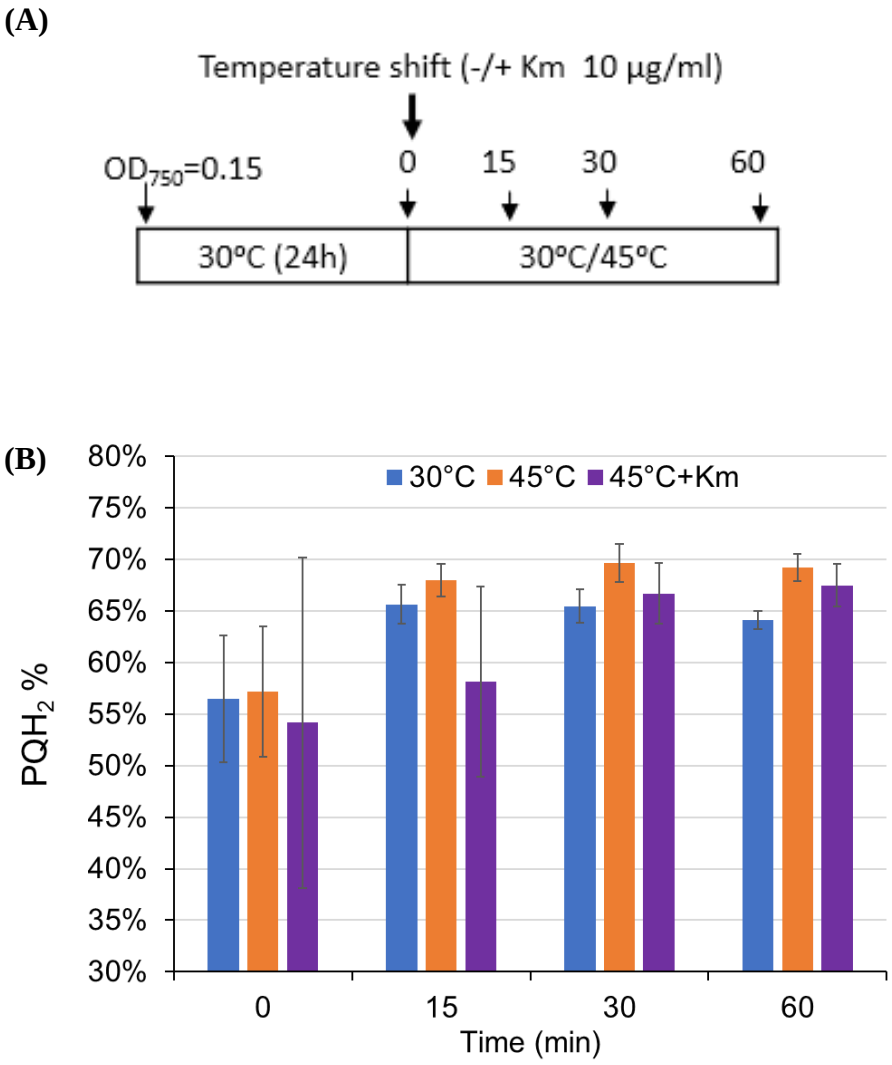

Fig. 4.4 Measurement of redox state of Plastoquinone pool under heat stress

(A) Experimental scheme. Cells were inoculated at an initial OD_{750} of about 0.15 in BG-11 liquid medium and incubated for 24 h. At the temperature upshift to 45°C, kanamycin (10 µg/ml) was added to the medium and cells were collected at indicated times for the analyses. **(B)** Redox state of plastoquinone pool was measured by HPLC analysis as described in (Khorobrykh et al. 2019).

4.4 Summary of Chapter 4

In this chapter, a comparison between heat inducible Rre1 phosphorylation and redox state of plastoquinone pool was shown. We found that the heat-induced phosphorylation of Rre1 decreased after a relatively short period (< 15 m), but this decrease did not occur when a protein synthesis inhibitor was present in the medium. This indicated that some newly synthesised protein(s) is required to shut off the response. Direct PQ pool measurement under high temperature showed that PQ pool become reduced after heat shock and remain reduced after 60 min, whereas Rre1 phosphorylation quenched at the same time. The kinetics of PQ pool redox state doesn't correlate with the Rre1 phosphorylation. In addition, under high temperature upshift in addition with a protein synthesis inhibitor, PQ pool became oxidized initially (Fig. 9) and comparing with the Rre1 phosphorylation in the same condition, Rre1 can be phosphorylated even if in PQ oxidized state. We concluded that Heat induction could induce Hik2 activity irrespective of PQ redox state. As Hik2 is redox responsive Fe-S protein, it is considerable that Fe-S cluster could itself change its redox state under heat induction irrespective of PQ redox change.

Chapter 5

Discussion

TCS is a signal transduction module predominantly found in bacteria, and several highly conserved components have been suggested to involve in divergent stress responses in cyanobacteria. Among them, Hik2 is an especially highly conserved histidine kinase and roles in high salt and hyperosmolarity stresses have been suggested in *Synechocystis* (Paithoonrangsarid et al. 2004, Shoumskaya et al. 2005), while the practical sensing and signaling mechanisms remain elusive because of the genetic essentiality and complex signaling network in the cell. In *S. elongatus*, it has been shown that the histidine kinase Hik2 interacts with and phosphorylates the response regulator Rre1 *in vitro* (Kato et al. 2012) and that Rre1 is responsible for the transcriptional activation of major chaperone and other protein genes by binding to these gene promoter regions (Kobayashi et al. 2017). Rre1 phosphorylation and the target genes transcription were enhanced in the cell during temperature upshift. However, deficiency of another conserved histidine kinase Hik34 resulted in diminish of these responses, and thus we previously concluded that the Rre1 dependent heat shock response is positively controlled by Hik34 (Kobayashi et al. 2017). In this study, we found that these diminished responses could be restored in the presence of secondary occurred suppressor mutations. Altogether, we here revise the working model as Hik2 phosphorylates Rre1 under stressed conditions and Hik34 is modulating this response.

The diminished Rre1 phosphorylation in the *hik34* mutant was restored by a miss-sense mutation of *rre1* (P114L), by a frame shift mutation in *sasA* (S83fs), and likely by a miss-sense mutation of *dnaK2* (R408C). Strains harboring only $rre1^{P114L}$ or $sasA^{83fs}$ mutation grew as rapid as the WT strain and showed restoration of the Rre1 phosphorylation and the *hspA* transcriptional activation under temperature upshift (Fig. 2.3). These results indicated that these mutations are epistatic to the *hik34* deletion mutation, and Rre1 and SasA are working at the downstream of Hik34 function. While events performed by these gene products for the Hik2-Rre1 signaling are unknown, we suggest that Rre1, SasA and probably DnaK2 are involved in

the repression of Hik2-dependent Rre1 phosphorylation, where Hik34 has a function to negate this repression. The histidine kinase SasA is known to interact with the circadian oscillator KaiC and modulates the RpaA dependent genome wide transcriptional oscillation. This suggests the circadian rhythm may affect the Hik2-Rre1 signaling event and the underlying regulatory scheme would be an interesting subject for future studies.

Other than the temperature upshift, Rre1 phosphorylation was also enhanced under PQ pool reducing condition but not under PQ pool oxidizing condition *in vivo* (Fig. 10C). This phosphorylation is very likely dependent on Hik2, and the responsiveness to the PQ pool redox status is well consistent with a previous report in *Synechocystis* (Ibrahim et al. 2020): Hik2 GAF domain is linked to a redox active [3Fe-4S] cluster through the conserved Cys residue, and the kinase activity is modulated by the redox change of the FeS cluster responding to the PQ pool redox status. We surely confirmed the conservation of the Cys residue in the Hik2 GAF domain (Fig. 3.1 and 3.2), supporting the same regulatory scheme in *S. elongatus*. However, there is an apparent contradiction between our result and the previous report: the Rre1 phosphorylation was enhanced under PQ pool reducing condition *in vivo* (Fig. 3.3C), whereas the Hik2 autophosphorylation was enhanced under PQ oxidizing condition *in vitro* (Ibrahim et al. 2020). In general, a specific His residue of histidine kinase is first auto phosphorylated and then this phosphate group is transferred to a conserved Asp residue of receiver domain of response regulator (Stock et al. 2000). While both phosphorylation events are usually considered to be activated or inactivated as a set, they are distinct reactions each other and thus it is possible to separately regulate the auto phosphorylation and subsequent phosphor transfer. Future biochemical analysis to reconstitute and monitor the Hik2 auto phosphorylation and the phosphor transfer to Rre1 is required to explain the apparent discrepancy. It is also of note that, under PQ pool oxidizing condition induced by DCMU, Rre1 phosphorylation was not observed while the *hspA* transcription was activated (Fig. 3.3B). This

may suggest that Rre1 still could activate the *hspA* transcription without phosphorylation or the presence of Rre1 independent activation pathway for the *hspA* transcription. These potential activation pathways are still hypothetical, but this study have unexpectedly revealed the complexity of the chaperone genes transcriptional regulation.

As described above, Rre1 phosphorylation and the downstream *hspA* transcriptional activation were observed under PQ pool reducing condition, which was considered to occur dependent on Hik2. Meanwhile, the underlying mechanism for the activation of the Hik2-Rre1 TCS under heat shock remains unknown, and it is not clear whether this mechanism is independent of or interconnected with the redox dependent regulation. In this study, we have obtained two lines of results to consider the relationship. Firstly, a prior addition of DCBQ to the medium completely abolished the heat induced response. This inhibition was not observed by addition of reduced DCBQ (Fig. 3.4), and thus oxidation of unidentified cellular molecule is likely involved for this. DCBQ was previously shown to oxidize Q_A of PSII and induce Q_B and PQ pool oxidation (Kashino et al. 1996, Schuurmans et al. 2014). As shown above, reduction of the Hik2-FeS cluster resulted from PQ reduction may activate the Rre1 phosphorylation. Therefore, it would be reasonable to assume that oxidation of the Hik2-FeS cluster, either mediated by PQ oxidation or by direct oxidation of the FeS cluster, prevented the heat induced Hik2 activation. Secondly, extraction and analysis of cellular PQ revealed that there is no apparent correlation between the heat inducible Rre1 phosphorylation and the PQ pool redox status (Figs. 4.1 and 4.3). Because Hik2 appears to be activated both under temperature upshift and PQ reducing conditions, it was possible to consider that the temperature upshift induced rapid PQ reduction, which then triggered that Hik2 activation. However, this scheme was unlikely the case because of the lack of the correlation. Rather, the oxidation of the FeS cluster appears to be inhibiting the heat inducible response. Based on these results, we are currently hypothesizing the Hik2 regulatory scheme as in Fig. 5. Under the

physiological conditions, PQ pool is mostly oxidized but small fraction is in the reduced state. Accordingly, a large part of Hik2-FeS cluster would be oxidized as well. The remaining reduced Hik2 is potentially able to phosphorylate Rre1, however, this activity is mostly repressed as described below and retained at the low level. After temperature upshift, the reduced form of Hik2 would be rapidly activated for the Rre1 phosphorylation by unknown mechanism, where transient loss of this repressing activity allows the rapid induction kinetics.

The heat induced Rre1 phosphorylation was declined after a relatively short period (< 15 m). We found this declination does not occur in the presence of protein synthesis inhibitor in the medium (Fig. 4.1), indicating some newly synthesized protein(s) is required to shut off the response. It was previously shown that expression of numbers of chaperone proteins are under the control of the phosphorylated Rre1 (Kobayashi et al. 2017). Thus, it is speculated that one or more of these proteins is involved in the negative feedback loop to repress the activation. In *Escherichia coli*, it is well known that a major chaperone protein DnaK is involved in the repression of the heat shock transcriptional activation, where DnaK interacts with the heat shock sigma factor s^{32} and results in the rapid degradation (Gamer et al. 1996). After temperature upshift, DnaK is titrated by heat-denatured proteins in the cell and thus released s^{32} is stabilized and activates heat shock protein genes including *dnaK*. The resultant accumulation of DnaK again results in the interaction with s^{32} to trigger the degradation and repress the heat shock response. The ortholog of *E. coli* DnaK is DnaK2 in *S. elongatus*, and the *dnaK2* gene is in fact under the control of Rre1 for the heat inducible expression (Kobayashi et al. 2017). While we have presently no evidence, the similar scheme involved an unidentified heat shock protein may well explain the kinetics of the observed responses.

The Hik2-Rre1 TCS module is highly conserved among cyanobacteria. The conserved Cys residue in the Hik2-GAF domain is also widely conserved (Fig. 3.1) and is likely involved in the redox sensing through the attached FeS cluster as suggested in this and previous studies

(Ibrahim et al. 2020). Meanwhile, Hik2 homologs from marine cyanobacteria apparently lack the conserved Cys residue (Fig. 3.1), and thus the similar redox sensing may not be occurring among this diverged cyanobacterial group (Scanlan et al., 2009). Further analysis is required to understand physiological roles of these Hik2 proteins, but it might be suggested that another role for heat shock response may explain the conservation of Hik2 homologs. Genes encoding the Hik2-Rre1 homologs, together with probable regulatory target genes *dnaK* and *groEL*, are also found from the chloroplasts of non-green lineages (Ohta et al. 2003). Thus, the regulatory scheme identified in cyanobacteria would be helpful to understand that in those chloroplasts. The nuclear encoded Hik2 homolog found in *Arabidopsis* chloroplast is chloroplast sensory kinase (CSK) that conserves the N-terminal GAF domain and the Cys residue (Puthiyaveetil and Allen 2009, Ibrahim et al. 2020). However, there is no evidence for the presence of Rre1 in plant chloroplasts, and information sensed by CSK is connected to regulate the SIG1-containing RNA polymerase activity (Puthiyaveetil et al. 2013). Here, the relevant TCS scheme was lost but the sensory function by Hik2 homologs is likely conserved during the long evolution of oxygen evolving photosynthesis.

Currently several research has been performed the increase the production of bioproducts from engineered photosynthetic organisms. The increasing of temperature in atmosphere and CO_2 emission are alarming concern for the Earth. Engineered photosynthetic organisms could be useful to produce useful bioproducts and as well as contribute to CO_2 fixation by producing in large scale in diverse condition. By elucidating the high temperature sensing mechanism of Hik2-Rre1 in cyanobacteria, more general knowledge of high temperature gene regulation could be derived and that could be used to improve the viability under diverse condition of cyanobacteria to perform photosynthesis more efficiently and for future biotechnological applications of photosynthetic organisms.

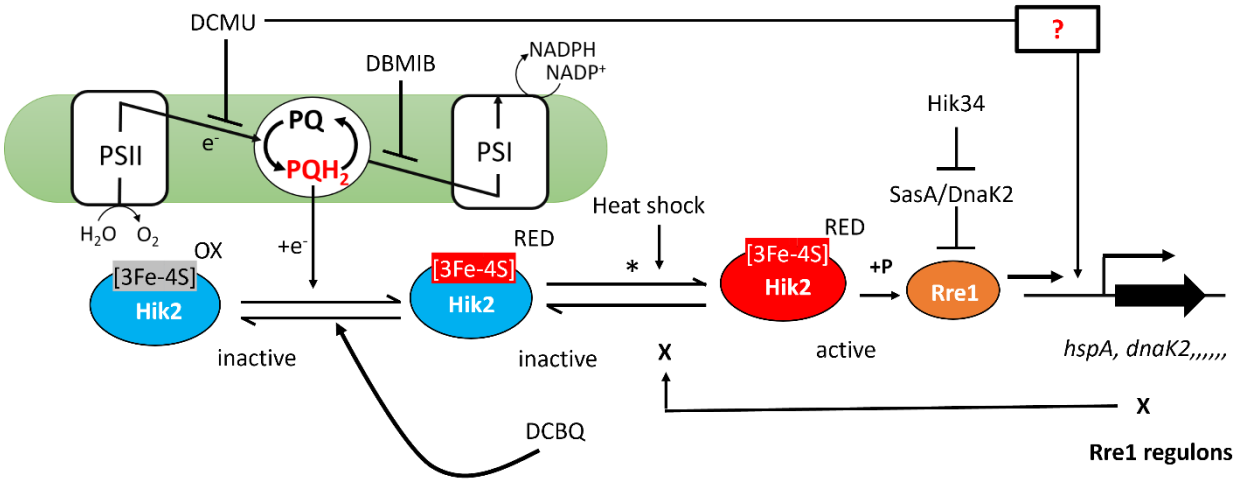

Fig. 5 Proposed model of the Hik2 activation for the Rre1 phosphorylation

Under standard growth conditions, FeS moiety attached with the Hik2 GAF domain is in equilibrium between reduced and oxidized forms, which changes the distribution responding to the PQ pool redox status of the photosynthetic electron transfer chain. The reduced form of Hik2 can change the conformation to activate the phosphate group transfer to Rre1, but this conformational change is reversed by the function of unknown chaperone protein X to keep the Rre1 phosphorylation very low level. Under temperature upshift, the reduced Hik2 rapidly changes the conformation for the activation of Rre1 phosphorylation, while the negating factor X is titrated by other heat denatured proteins to allow the strong Hik2 activation. After temperature upshift, the Rre1-dependent X gene expression is enhanced to result in its accumulation, which finally quenches the Hik2 activity and the Rre1 phosphorylation. DCBQ may oxidize and diminish the reduced Hik2 directly or indirectly, which prevents the Hik2 activation response after temperature upshift. In the hik34 deletion mutant, Rre1 phosphorylation by Hik2 is inhibited by the function of SasA and probably DnaK2. This

inhibition was restored by the mutations found in *sasA*, *rre1* or *dnaK2* genes, suggesting gene products are working downstream of Hik34.

References

Archibald, J.M. (2009) The puzzle of plastid evolution. *Current Biol.* 19: R81-R88.

Ashby, M.K., Houmard, J. (2006) Cyanobacterial two-component proteins: structure, diversity, distribution, and evolution. *Microbiol. Mol. Biol. Rev.* 70: 472-509.

Barber, J. (2008) Photosynthetic generation of oxygen. Philosophical Transactions of the Royal Society B: *Biological Sci.* 363: 2665-2674.

Bhattacharya, D., Yoon, H.S., Hackett, J.D. (2004) Photosynthetic eukaryotes unite endosymbiosis connects the dots. *Bioessays* 26: 50-60.

Blankenship, R.E. (2010) Early evolution of photosynthesis. *Plant physiol.* 154: 434-438.

Buick, R. (2008) When did oxygenic photosynthesis evolve? Philosophical Transactions of the Royal Society B: *Biological Sci.* 363:2731-2743.

Cohen, Y., Jørgensen, B.B., Revsbech, N.P., Poplawski, R. (1986) Adaptation to hydrogen sulfide of oxygenic and anoxygenic photosynthesis among cyanobacteria. *Appl. Environ. Microbiol.* 51: 398-407.

Doolittle, R.F., Feng, D.F., Tsang, S., Cho, G. and Little, E. (1996.) Determining divergence times of the major kingdoms of living organisms with a protein clock. *Science* 271: 470-477.

Ermakova, M., Huokko, T., Richaud, P., Bersanini, L., Howe, C.J., Lea-Smith, D.J., et al. (2016) Distinguishing the roles of thylakoid respiratory terminal oxidases in the cyanobacterium *Synechocystis sp*. PCC 6803. *Plant Physiol.* 171: 1307-1319.

Field, C.B., Behrenfeld, M.J., Randerson, J.T., Falkowski, P. (1998) Primary production of the biosphere: integrating terrestrial and oceanic components. *Science* 281: 237-240.

Gamer, J., Multhaup, G., Tomoyasu, T., McCarty, J.S., Rüdiger, S., Schönfeld, H.J., et al. (1996) A cycle of binding and release of the DnaK, DnaJ and GrpE chaperones regulates activity of the *Escherichia coli* heat shock transcription factor sigma32. *EMBO J.* 15: 607-617.

Hanaoka, M., Tanaka, K. (2008) Dynamics of RpaB–promoter interaction during high light stress, revealed by chromatin immunoprecipitation (ChIP) analysis in *Synechococcus elongatus* PCC 7942. *Plant J.* 56: 327-335.

Hasegawa, H., Tsurumaki, T., Kobayashi, I., Imamura, S., Tanaka, K. (2020) Identification and analysis of a principal sigma factor interacting protein SinA, essential for growth at high temperatures in a cyanobacterium *Synechococcus elongatus* PCC 7942. *J. Gen. Appl. Microbiol*. 66: 66–72.

Hosokawa, N., Hatakeyama, T.S., Kojima, T., Kikuchi, Y., Ito, H., Iwasaki, H. (2011) Circadian transcriptional regulation by the posttranslational oscillator without de novo clock gene expression in *Synechococcus*. *Proc. Natl. Acad. Sci. USA* 108: 15396-15401.

Ibrahim, I.M., Puthiyaveetil, S., Allen, J.F. (2016) A two-component regulatory system in transcriptional control of photosystem stoichiometry: redox-dependent and sodium ion-dependent phosphoryl transfer from cyanobacterial histidine kinase Hik2 to response regulators Rre1 and RppA. *Front. Plant Sci.* 7: 137.

Ibrahim, I.M., Wu, H., Ezhov, R., Kayanja, G.E., Zakharov, S.D., Du, Y., et al. (2020) An evolutionarily conserved iron-sulfur cluster underlies redox sensory function of the Chloroplast Sensor Kinase. *Commun. Biol.* 3: 1-11.

Iwasaki, H., Williams, S.B., Kitayama, Y., Ishiura, M., Golden, S.S., Kondo, T. (2000) A KaiC-interacting sensory histidine kinase, SasA, necessary to sustain robust circadian oscillation in cyanobacteria. *Cell* 101: 223-233.

Kanehisa, M., Furumichi, M., Tanabe, M., Sato, Y. and Morishima, K. (2017). KEGG: new perspectives on genomes, pathways, diseases and drugs. *Nucleic acids res.* 45: D353-D361.

Kappell, A.D., van Waasbergen, L.G. (2007) The response regulator RpaB binds the high light regulatory 1 sequence upstream of the high-light-inducible *hliB* gene from the cyanobacterium *Synechocystis* PCC 6803. *Arch. Microbiol.* 187: 337-342.

Kashino, Y., Yamashita, M., Okamoto, Y., Koike, H. and Satoh, K. (1996) Mechanisms of electron flow through the QB site in Photosystem II. 3. Effects of the presence of membrane structure on the redox reactions at the QB site. *Plant cell physiol.* 37: 976-982.

Kato, H., Watanabe, S., Nimura-Matsune, K., Chibazakura, T., Tozawa, Y., Yoshikawa, H. (2012) Exploration of a possible partnership among orphan two-component system proteins in cyanobacterium *Synechococcus elongatus* PCC 7942. *Biosci. Biotechnol. Biochem.* 76: 1484-1491.

Khorobrykh, S., Tsurumaki, T., Tanaka, K., Tyystjärvi, T., Tyystjärvi, E. (2020) Measurement of the redox state of the plastoquinone pool in cyanobacteria. *FEBS Lett.* 594: 367-375.

Kim et al. 2015 is "Kim, Y.I., Boyd, J.S., Espinosa, J. and Golden, S.S. (2015) Detecting KaiC phosphorylation rhythms of the cyanobacterial circadian oscillator in vitro and in vivo. *Meth. enzymol.* 551: 153-173.

Kirby, K.S., Fox-Carter, E., Guest, M. (1967) Isolation of deoxyribonucleic acid and ribosomal ribonucleic acid from bacteria. *Biochem. J.* 104: 258-262.

Kobayashi, I., Watanabe, S., Kanesaki, Y., Shimada, T., Yoshikawa, H., Tanaka, K. (2017) Conserved two-component Hik34-Rre1 module directly activates heat-stress inducible transcription of major chaperone and other genes in *Synechococcus elongatus* PCC 7942. *Mol. Microbiol.* 104: 260-277.

Kurisu, G., Zhang, H., Smith, J.L. and Cramer, W.A. 2003) Structure of the cytochrome b6f complex of oxygenic photosynthesis: tuning the cavity. *Science* 302: 1009-1014.

Lee, S., Prochaska, D.J., Fang, F., Barnum, S.R. (1998) A 16.6-kilodalton protein in the cyanobacterium *Synechocystis* sp. PCC 6803 plays a role in the heat shock response. *Curr. Microbiol.* 37: 403-407.

Mascher, T., Helmann, J.D., Unden, G. (2006) Stimulus perception in bacterial signal-transducing histidine kinases. *Microbiol. Mol. Biol. Rev.* 70: 910-938.

Mironov, K.S., Los, D.A. (2015) RNA isolation from *Synechocystis*. *Bio-protocol* 5: e1428.

Moronta-Barrios, F., Espinosa, J., Contreras, A. (2012) *In vivo* features of signal transduction by the essential response regulator RpaB from *Synechococcus elongatus* PCC 7942. *Microbiology* 158: 1229-1237.

Nakamura, Y., Kaneko, T., Hirosawa, M., Miyajima, N., Tabata, S., (1998). CyanoBase, a www database containing the complete nucleotide sequence of the genome of *Synechocystis* sp. strain PCC6803. *Nucleic acids res.* 26: 63-67.

Ohta, N., Matsuzaki, M., Misumi, O., Miyagishima, S.Y., Nozaki, H., Tanaka, K., et al. (2003) Complete sequence and analysis of the plastid genome of the unicellular red alga *Cyanidioschyzon merolae*. *DNA Res.* 10: 67-77.

Olson, J.M.,Blankenship, R.E. (2005) Thinking about the evolution of photosynthesis. *Discoveries in Photosynthesis*: 1073-1086.

Paithoonrangsarid, K., Shoumskaya, M.A., Kanesaki, Y., Satoh, S., Tabata, S., Los, D.A., et al. (2004) Five histidine kinases perceive osmotic stress and regulate distinct sets of genes in *Synechocystis*. *J. Biol. Chem.* 279: 53078-53086.

Pruitt, K.D., Tatusova, T., Maglott, D.R. (2007). NCBI reference sequences (RefSeq): a curated non-redundant sequence database of genomes, transcripts and proteins. *Nucleic acids res.* 35: D61-D65.

Puthiyaveetil, S., Allen, J.F. (2009) Chloroplast two-component systems: evolution of the link between photosynthesis and gene expression. *Proc. Royal Soc. B: Biol. Sci.* 276: 2133-2145.

Puthiyaveetil, S., Ibrahim, I.M., Allen, J.F. (2013) Evolutionary rewiring: a modified prokaryotic gene-regulatory pathway in chloroplasts. *Phil. Trans. Royal Soc. B: Biol. Sci.* 368: 20120260.

Rabinowitch, Eugene (1960 Action spectrum of the “second Emerson effect”. *Biophys. J.* 1.2: 73-89.

Rippka, R. (1988) [1] Isolation and purification of cyanobacteria. *Methods Enzymol.* 167: 3-27.

Rubin, B.E., Wetmore, K.M., Price, M.N., Diamond, S., Shultzaberger, R.K., Lowe, L.C., et al. (2015) The essential gene set of a photosynthetic organism. *Proc. Natl. Acad. Sci. USA.* 112: E6634-E6643.

Sato, S., Shimoda, Y., Muraki, A., Kohara, M., Nakamura, Y., Tabata, S. (2007) A large-scale protein–protein interaction analysis in *Synechocystis* sp. PCC 6803. *DNA Res.* 14: 207-216.

Scanlan, D.J., Ostrowski, M., Mazard, S., Dufresne, A., Garczarek, L., Hess, W.R., et al. (2009) Ecological genomics of marine picocyanobacterial. *Microbiol. Mol. Biol. Rev.* 73: 249-299.

Schultz, J., Copley, R.R., Doerks, T., Ponting, C.P., Bork, P (2000). SMART: a web-based tool for the study of genetically mobile domains. *Nucleic acids res.* 28: 231-234.

Schuurmans, R.M., Schuurmans, J.M., Bekker, M., Kromkamp, J.C., Matthijs, H.C. et al. (2014) The redox potential of the plastoquinone pool of the cyanobacterium *Synechocystis* species strain PCC 6803 is under strict homeostatic control. *Plant Physiol.* 165: 463-475.

Sechbach, J., Oren, A. (2007) Oxygenic photosynthetic microorganisms in extreme environments: Possibilities and limitations: In Algae and cyanobacteria in extreme environments (Vol. 11). Edited by Sechbach, J. pp. 5-25. Springer Science & Buisiness Media, New York City, USA.

Seki, A., Hanaoka, M., Akimoto, Y., Masuda, S., Iwasaki, H. and Tanaka, K. (2007) Induction of a group 2 σ factor, RPOD3, by high light and the underlying mechanism in Synechococcus elongatus PCC 7942. *J. Biol. Chem*. 282: 36887-36894.

Shoumskaya, M.A., Paithoonrangsarid, K., Kanesaki, Y., Los, D.A., Zinchenko, V.V., Tanticharoen, M., et al. (2005) Identical Hik-Rre systems are involved in perception and transduction of salt signals and hyperosmotic signals but regulate the expression of individual genes to different extents in *Synechocystis. J. Biol. Chem.* 280: 21531-21538.

Slabas, A.R., Suzuki, I., Murata, N., Simon, W.J., Hall, J.J. (2006) Proteomic analysis of the heat shock response in *Synechocystis* PCC 6803 and a thermally tolerant knockout strain lacking the histidine kinase 34 gene. *Proteomics* 6: 845-864.

Stock, A.M., Robinson, V.L., Goudreau, P.N. (2000) Two-component signal transduction. *Annu. Rev. Biochem.* 69: 183-215.

Suzuki, I., Kanesaki, Y., Hayashi, H., Hall, J.J., Simon, W.J., Slabas, A.R. and Murata, N. (2005) The histidine kinase Hik34 is involved in thermotolerance by regulating the expression of heat shock genes in Synechocystis. *Plant Physiol.* 138: 1409-1421.

Takai, N., Nakajima, M., Oyama, T., Kito, R., Sugita, C., Sugita, M., et al. (2006) A KaiC-associating SasA–RpaA two-component regulatory system as a major circadian timing mediator in cyanobacteria. *Proc. Natl. Acad. Sci. USA.* 103: 12109-12114.

Thompson, J.D., Higgins, D.G.,Gibson, T.J. (1994). CLUSTAL W: improving the sensitivity of progressive multiple sequence alignment through sequence weighting, position-specific gap penalties and weight matrix choice. *Nucleic acids res.* 22: 4673-4680.

Vidal, R., López-Maury, L., Guerrero, M.G., Florencio, F.J. (2009) Characterization of an alcohol dehydrogenase from the cyanobacterium *Synechocystis* sp. strain PCC 6803 that responds to environmental stress conditions via the Hik34-Rre1 two-component system. *J. Bacteriol.* 191: 4383-4391.

Waterbury, J.B., Watson, S.W., Guillard, R.R., Brand, L.E. (1979) Widespread occurrence of a unicellular, marine, planktonic, cyanobacterium. *Nature* 277: 293-294.

Zehr, J.P. (2011) Nitrogen fixation by marine cyanobacteria. *Trends Microbiol.* 19: 162-173

Supplemental Data

Table S1. Strains and plasmids used in this study

Strain	Genotype or relevant characteristics	Source
WT	*Synechococcus elongatus* PCC 7942 (Wild-type)	Laboratory stock
NB94	Synpcc7942_1517*::kan*	This study
SU92	Synpcc7942_1517*::kan*, *dnaK2*^{R480C}	This study
SU94	Synpcc7942_1517*::kan*, *rre1*^{P114L}	This study
SU103	Synpcc7942_1517*::kan*, *sasA*^{S83fs}	This study
R94	Synpcc7942_1860*::* *rre1*^{P114L}, *Spr*	This study
S103	Synpcc7942_2114*::* *sasA*^{S83fs}, *Spr*	This study
RH94	Synpcc7942_1517*::kan*	This study
	Synpcc7942_1860:: *rre1*^{P114L}, *Spr*	
SH103	Synpcc7942_1517*::kan*	This study
	Synpcc7942 2114:: *sasA*^{S83fs}, *Spr*	
R-F	Synpcc7942_1860-3 x FLAG-tag, *Spr*	Kobayashi et al. 2017
HSK	Synpcc7942_2401*::kan*	This study

Plasmid	Genotype or relevant characteristics	Source
pBΩH	pBluescript with omega fragment, *Spr*	Hasegawa et al. 2019
pBΩH-D92	pBΩH with *dnaK2*^{R480C}	This study
pBΩH-R94	pBΩH with *rre1*^{P114L}	This study
pBΩH-S103	pBΩH with *sasA*^{S83fs}	This study

Table S2. Primer used in this study

Name	**Sequence (5'→3')**
For cloning	
dnaK2-Fw-SacI	ggaGAGCTCatggccaaagttgtcggaatcg
dnaK2-Rv-BamHI-SmaI	ggaCCCGGGGGATCCttacttcgactcagagaactctgcgt
2469-Fw-SalI	ggaCCCGGGGTCGACtcacctaggcagtttgggaatgaa
2469-Rv-KpnI	ggaGGTACCgaatcgggaccgccagg
sasAUp-F-SacI	ggaGAGCTCctcgtgccttcgccaaga
sasA-Rv-NotI	aggGCGGCCGCttagcagggcatggtgtagc
sasADN-FW-XhoI	aggCTCGAGcgcaccgcgatcgcggtc
sasADN-RV-KpnI	aggGGTACCtgagattgctcaacaactctttctggc
rre1-Fw-NotI	GCGGCCGCtcaatcagctaggccatgctc
rre1-Rv-BamHI	aggGGATCCatggagcaagctgtgagcg
rre1DN-Fw-XhoI	aggCTCGAGgctcgttctcagtctagtgc
rre1DN-RV-KpnI	aggGGTACCcctcaagcgttatcaagagcg
Mutant construction	
hik34-F	CGCTAGCTGGTTGAGCTTTT
hik34-R	CGGTCTTTCTGCTCTGTTCC
2402dn-EcoRI-Fw	gaaGAATTCcaatccagcagtcgcagcc
2402dn-Km-Rw	ttttgagacacaacgtggcttttgaggtctccctaacggactg
2400up-Km-Fw	tccacctacaacaaagctctcgccatccacgttgagtcc
2400up-HindIII-Rw	gaaAAGCTTtctagttcgacacgaattgtggtgc
KmR-Fw	AGCCACGTTGTGTCTCAAAATCTCTGATGT
KmR-Rw	AGAGCTTTGTTGTAGGTGGACCAGTTGGTG

Probe preparation for northern blotting

hspA-Prb-Fw	atggcactcgttcgattcagtcc
hspA-Prb-Rv	ctatcgctcgcaagcttcagc
rnpB-Prb-Fw	gtgaggagagtgccacagaa
rnpB-Prb-Rw	taagccgggttctgttctct

BG-11 Media Preparation

For liquid BG-11

Solution (Vol.)	**Vol.**	
Stock solution 1 (ml)	50	
Stock solution 2 (µl)	1	*
Stock solution 3 (µl)	1	*
Stock solution 4 (µLl)	1	*
Stock solution 6 (µl)	1	*
Micro element A6 (µl)	1	*
1M HEPES KOH pH 8.0 (ml)	20	*
H_2O (ml)	925	
Total (ml)	1,000	

Autoclave (121°C,15 min) *add after autoclave

For BG-11 plate

Solution (Vol.)	Vol.	
Stock solution 1 (ml)	15	
Stock solution 2 (µl)	300	*
Stock solution 3 (µl)	300	*
Stock solution 4 (µl)	300	*
Stock solution 5 (µl)	300	*
Stock solution 6 (µl)	300	*
Micro element A6 (µl)	300	*
1M HEPES KOH pH 8.0 (ml)	6	
H_2O (ml)	277.5	
Agar (g)	4.5	
Total (ml)	300	

Autoclave (121°C,15 min) *add after autoclave

BG-11 Stock Solutions

Stock solution 1 (20×)

Component	Molecular Mass	Amount (g)
Na_2NO_3 (Sodium Nitrate)	84.99	30
$MgSO_4 \cdot 7H_2O$ (Magnesium Sulfate Heptahydrate)	246.47	1.5

Total volume to 1,000 ml

Autoclave (121°C,15 min)

Stock solution 2 (1000×)

Component	Molecular Mass	Amount (g)
Citric Acid·H_2O	210.14	0.6
Ammonium Iron (III) Citrate, Brown	261.98	0.6
$Na_2EDTA \cdot 2H_2O$	372.24	0.1

Total volume to 100 ml Fertilize by filter (0.22 μm) and store at 4ºC

Stock solution 3 (1000×)

Component	Molecular Mass	Amount (g)
$CaCl_2 \cdot 2H_2O$ (Calcium Chloride Dihydrate)	147.01	3.7

Total volume to 1,000 ml Autoclave (121°C,15 min)

Stock solution 4 (1000×)

Component	Molecular Mass	Amount (g)
Na_2CO_3 (Sodium Carbonate)	105.9885	2.0

Total volume to 1,000 ml

Autoclave (121°C, 15min)

Stock solution 5 (1000×)

Component	Molecular Mass	Amount (g)
$Na_2S_2O_3$ (Sodium Thiosulfate)	158.11	15.8

Total volume to 1,000 ml

Autoclave (121°C,15 min)

Stock solution 6 (1000×)

Component	Molecular Mass	Amount (g)
K_2HPO_4 (Potassium Hydrogen Phosphate)	174.18	3.8

Total volume to 1,000 ml Autoclave (121°C,15 min)

1M HEPES -KOH (pH 8.0) (50×)

Component	Molecular Mass	Amount (g)
HEPES	238.3012	238.3

* Adjust pH to 8.0 with KOH (Potassium Hydroxide)

Total volume to 1,000 ml Autoclave (121°C,15 min)

Microelements A6 (1000×)

Component	Molecular Mass	Amount (g)
H_3BO_3 (Boric Acid)	61.83	2.86
$MnCl_2·4H_2O$ (Manganese (II) Chloride Tetrahydrate)	197.9	1.81
$ZnSO_4·7H_2O$ (Zinc Sulfate Heptahydrate)	287.56	0.222
$Na_2MoO_4·2H_2O$ (Sodium Molybdate Dihydrate)	241.95	0.39
$CuSO_4·5H_2O$ (Copper Sulfate Pentahydrate)	249.68	0.079
Co $(NO_3)_2·6H_2O$ (Cobaltous Nitrate Hexahydrate)	291.03	0.0494

Total volume to 1,000 ml and store at 4ºC

Basic PCR Procedure

PCR mixture

KOD plus Neo PCR buffer (10×)	2 µl
dNTPs (2 mM)	2 µl
MgSO4 (25 µM)	1.2 µl
DNA template (10 ng)	0.4 µl
Primer-F (10 pmol/µl)	0.6 µl
Primer-R (10 pmol/µl)	0.6 µl
KOD plus Neo polymerase	0.4 µl
H_2O	12.8 µl
Total	20 µl

PCR reaction cycle

Temp.	Time (min)	
94ºC →	2:00	
98ºC →	0:30	30 cycles
60ºC →	0:30	
68ºC →	2:30	
68ºC →	5:00	

Colony PCR

PCR mixture

GoTaq PCR master mix	5 µl
Primer-F (10 pmol/µl)	0.2 µl
Primer-R (10 pmol/µl)	0.2 µl
H_2O	4.6 µl
Total	10 µl

PCR mixture distributed in PCR reaction tubes and added cells with a toothpick in to PCR reaction tube

Colony PCR reaction cycle

Temp.	Time (min)
95ºC →	2:00
95ºC →	0:30
60ºC →	0:30

72ºC ⟶ 4:30
72ºC ⟶ 5:00

30 cycles

Transformation of *hik34*::Km in to *S. elongatus*

S. elongatus cells were inoculated in BG-11 liquid medium at 30ºC with 2% CO_2 aeration under continuous fluorescent light (20 µmol photon/m^2/sec) and incubated until the OD_{750} reached above 1.

↓

5 ml culture were centrifuged at 5000rpm in 25ºC and resuspended the pellets with fresh BG-11 liquid media. 1 ml culture were transferred into Eppendorf tube and used for transformation.

↓

1 µg *hik34*::Km DNA cassette were added into 1 ml of cells for transformation and Eppendorf tube was covered with aluminum foil and incubated in dark for overnight.

↓

Cells were transferred to light after dark incubation for at least 2 hours.

↓

After 2 hours, cells were centrifuged at 5,000 rpm for 1 min and discarded excess supernatant.

↓

Cells were resuspended by micro pipette and platted on a BG-11 solid medium containing 10 µg/ml of kanamycin.

RNA Extraction from Cyanobacteria (Hot phenol method)

RNA extraction buffer

Components	Conc.	Amount
50mM Tris-HCl (pH 6.5)	Stock: 1 M	2.5 ml
5mM EDTA (pH 8.0)	Stock: 0.5 M	0.5 ml
0.5%(w/v) SDS		0.25 g
H_2O (RNA grade)		47.5 ml
		Total 50 ml

Collect cyanobacteria from liquid culture 10 ml (OD_{750} = 0.4 – 0.6) in 50 ml collection tube

7,000 x g, 2 min, 4 ℃

Resuspend the pellet by 1 ml BG-11 (supernatant) and transfer to 1.5 ml tube

15,000 rpm, 15 sec, 4 ℃

Discard the supernatant and store the pellet at -80 ℃

Add RNA extraction buffer 450 µl and mix by Vortex completely

Add acidic phenol (RNA grade) 450 µl (equal volume) and mix by inverting 4 – 6 times

15,000 rpm, 5 min, RT

Take supernatant to new 1.5 ml tube

Add PCI (RNA grade) 400 µl and mix by inverting 4 – 6 times

15,000 rpm, 5 min, RT

Take supernatant to new 1.5 ml tube

Add PCI (RNA grade) 400 µl and mix by inverting 4 – 6 times

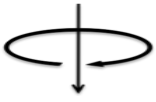

15,000 rpm, 5 min, RT

Take 80 % supernatant to new 1.5 ml tube (avoid white pellet)

Add 5 M LiCl 1/10 volume (about 40 µl)

Add 100 % EtOH 2 – 2.5 volume (about 1 ml)

Store at – 30 ℃for 15 min

 15,000 rpm, 30 min, 4 ℃

Discard the supernatant

Add 70 % EtOH (RNA grade) 300 µl

 15,000 rpm, 5 min, 4 ℃

Discard the supernatant and dry up on the bench

↓

Resolve the RNA pellet by H_2O (RNA grade) 40 µl

↓

Measure the concentration by Nanodrop

Northern Blotting Analysis

Solutions for Northern Blotting

20× SSC

Components	**Conc.**	**Amount (g)**
NaCl	3.0 M	350.6 g
Trisodium Citrate Dihydrate	0.30 M	174.46 g
MiliQ water		up to 2,000 ml

Autoclave 121ºC, 40 min

10×MOPS Buffer (Running Buffer）

Components	Conc.	Amount (g)
MOPS	200 mM	41.9 g
Sodium acetate	50 µM	6.8 g
EDTA	10 mM	3.72 g
MiliQ water		up to 1,000 ml

Autoclave 121 ℃, 40 min

10×Buffer 1

Components	Conc.	Amount (g)
Maleic acid	1.0 M	116.07 g
NaCl	1.5 M	87.66 g
MiliQ water		up to 1,000 mL

Autoclave 121 ℃, 40 min

10 x Blocking stock solution (10 %)

Components	Amount
Blocking Reagent （Roche）	10 g
1 x Buffer 1	90 ml

Autoclave 121 ℃, 15 min and store at -20 ℃

Wash Buffer

Components	Amount
1×Buffer1	1,000 ml
tween-20 (Sigma)	0.3 %

Buffer 2

Components	Amount
10 x Blocking stock solution	5 ml
1×Buffer1	45 ml

10 x Buffer3 (Detection buffer)

Components	Conc.	Amount (g)
Trizma base	1 M	60.5 g
NaCl	1 M	29.22 g
$MgCl_2$	0.5 M	23.8 g
MiliQ		up to 500 ml

Adjust pH 9.5 by NaOH Autoclave 121 ℃, 40 min

Use 1 x concentration by diluting with MiliQ

RNA Sample mix

10×MOPS Buffer：formaldehyde：formamide ＝ 2 ml：3 ml：10 ml

Store at 4 ℃

Methylene blue solution

Sodium acetate	4.1 g (0.5 M)
Methylene blue	0.04%
MiliQ	up to 100 ml

Hybridization Buffer

Components	**Amounts**
20×SSC	25 ml
Formamide	50 ml
2M Sodium phosphate Buffer	2.5 ml
10 x Blocking stock solution	20 ml
10% N- Lauroylsarcosine	1 ml
SDS	7 g
Yeast total RNA	5 mg
MiliQ	up to 100 ml

Low stringency Buffer (100 mL)

2×SSC	10 ml
0.1%SDS	1 ml
H_2O	89 ml

High stringency Buffer (100 mL)

0.5×SSC	2.5 ml
0.1%SDS	1 ml
H_2O	96.5 ml

1.0% denature agarose gel

10×MOPS Buffer	10 ml
Agarose ME	1.0 g
MiliQ	87 ml

Melt agarose by microwave and cool down about 50℃, add formaldehyde 3 ml

Northern Blotting

1. Prepare RNA sample

3 µg RNA with H_2O	7.5 µl
RNA sample mix	7.5 µl
Total	15 µl

Incubate 65ºC for 10min

Rapid cooling for 2 min on ice

Add 10 x RNA Loading buffer 1.5 µl

2. Load samples to 1.0 % denature agarose gel and electrophoresis in 1 x MOPS buffer (up to the first dye reach to forth line of gel plate from bottom) for 40 min at 100V power supply.

3. Preparing Blotter

Container for Northern blot

Stand for Northern blot

From bottom, prepare	3 sheets Whatman 3MM (12 cm x 25 cm)
	3 sheets
	Gel (block gel side by Saran wrap)
	Membrane
	3 sheets Whatman 3MM (12 cm x 12 cm)
	Comfort towel (11 cm x11 cm)

Pore 20×SSC to container and remain overnight for transferring RNA to membrane.

4. Remove the membrane from Blotter, and crosslink by UV (1200×100 mJ/cm^2).

5. Stain by Methylene blue solution and wash by MiliQ.

6. Pack the membrane in hybrid-pack and add hybridization buffer 12 ml/ Incubate at 48℃ for 30 min.

7. Incubate DNA probe at 65℃ 5 min and rapid cool for 3 min on ice.

8. Add DNA probe for hybridization buffer (500~1000 ng/ml) Incubate at 48℃ O/N.

9. Transfer hybridization buffer in a collection tube and store at -30℃ (able to reuse).

10. Wash membrane by low stringency buffer at RT 5 min X 2.

11. Wash membrane by high stringency buffer at 68℃ 15 min X 2.

12. Wash membrane by wash buffer briefly.

13. Incubate in buffer 2 RT 1 h.

14. Add DIG-AP antibody (Roche) 1/10000 vol. against buffer 2 vol. Incubate at RT 30 min ~ 1 h (*able to reuse).

15. Wash membrane by wash buffer at RT 15 min X 2.

16. Equilibrate membrane in Buffer3 for 3min.

17. Prepare Sran wrap and put the membrane Drop CDP-star ready-to-use (Roche) 7 or 8 drops equally and incubate at RT 5 min **i**n dark.

18. Detect the expression by lumminograph.

DIG-labelled DNA probe preparation

PCR reaction

KOD plus Neo PCR buffer (10×)	2 µl
DIG-dNTPs (2 mM)	2 µl
MgSO4 (25 µM)	1.2 µl
DNA template (10 ng)	0.4 µl
Primer-F (10 pmol/µl)	0.6 µl
Primer-R (10 pmol/µl)	0.6 µl
KOD plus Neo polymerase	0.4 µl
H_2O	12.8 µl
Total	20 µl

Temp.	Time	
94ºC	2:00	
98ºC	0:30	40 cycles
60ºC	0:30	
68ºC	0:30	
68ºC	5:00	

Add 500~1000 ng DIG-labelled DNA into 50 ml Buffer solution 2 and stored at 4ºC.

Phos-tag SDS PAGE

Sampling

1. Collect cyanobacteria from liquid culture 10 ml (OD_{750} = 0.4 – 0.6) in 50 ml collection tube 7,000 x g, 2 min, 4 ℃.

2. Discard the supernatant, resuspend in 1 ml of TBS for ChIP that had been chilled on ice, and transfer to a 1.5 ml tube.

3. Centrifuge 4 ℃, 15000 rpm, 15 sec.

4. Remove supernatant and store pellets at liquid Nitrogen until protein extraction.

Protein extraction

1. Resuspend the cell pellet in 100 µL of lysis buffer (25 mM Tris pH 8.0, 0.5 mM

EDTA and sterilized deionized water). Add glass beads (Acid washed 425-600 µm diameter) equivalent to one-third of the volume. Cells can be lysed using a benchtop vortex at maximum setting with ten cycles alternating 30 seconds vertexing/30 seconds cooling on ice.

2. Centrifuge cell extract at 10 000 × g for 5 min at 4ºC to pellet unbroken cells, cellular debris, and beads. Transfer the blue-green supernatant to a new tube and use an aliquot to quantify protein concentration using a Bradford assay. Samples should be used immediately for gel loading.

Phos-Tag gel preparation

1. Clean the gel making apparatus with 70% ethanol and seal the apparatus well to prevent the leakage.

2. Except TEMED, reagents of separating were mixed at a proportion of 8% shown in the table. Reagents of stacking gel were mixed as per the number of gels. TEMED should not be mixed in this case also.

3. Pour Separating gel, which is a mixture of TEMED and 10% APS, to a height of about 6 cm. The rest of the space was filled with 70% ethanol. Phos-Tag containing gel must be keep under dark.

4. When the Separating gel has hardened, wash the layered ethanol thoroughly.

5. 10% APS mixed with stacking gel mixture and poured to top of the separating gel, set the comb (10 well comb is recommended). The gel must be kept at dark until hardened.

6. After the Stacking gel has hardened, remove the comb and seal tube, and wash the wells with his SDW. The gel should be attached to electrophoresis apparatus and kept under dark at 4^{o}C until loading the protein for electrophoresis.

Electrophoresis and Blotting

1. Load 20 μg of protein extract in 1XSDS sample buffer per lane (for Rre1 detection) and run at 100V, 12 mA at 4^{o}C for approximately 3 hours in a Tris/Glycine/SDS buffer.

2 Incubate gels twice for 10 min at RT in transfer buffer solution (Tris/Glycine/ Methanol supplemented with 10 mM EDTA), then twice more in standard transfer solution without EDTA for 5 min.

3. Transfer proteins from gel to PVDF membrane by wet electroblotting (tank transfer). Transfer at 1 mA/cm^2 for 60 min at room temperature.

4. Block the membrane with 2.5% nonfat dry milk (Skim milk)/Tris-buffered saline (TBS) + 0.1% Tween-20 for 1 hour at RT and then incubate with Anti-Rre1 (1:4000) for 1 hour at room temperature on a rotary shaker.

5. Then, rinse the membrane three times with 1XTBS-T for 10 min.

6. After washing the membrane, incubate the membrane with Anti-Rabbit-HRP-linked secondary antibody (1: 4000) in Skim milk/TBS-T for 30 min.

7. Then, wash the membrane three times with 1XTBS-T for 10 min,

8. Place the membrane on the film and use ImmunoStar Zeta (Wako) Solution A and Solution Drop a 1: 1 mixture of B and detect chemiluminescence with LuminoGraph I (ATTO).

Separating gel for Phos-Tag SDS-PAGE	25 µM Phos-tag X % gel				Vol
Component	6	8	10	12	mL
30**%** acrylamide	1.2	1.6	2	2.4	mL
4x Separating Buffer	1.5	1.5	1.5	1.5	mL
H2O	3.17	2.77	2.37	1.97	mL
5 mM Phos-tag	30	30	30	30	µL
10 mM $MnCl_2$	30	30	30	30	µL
10**%**APS	60	60	60	60	µL
TEMED	6	6	6	6	µL
Total	6	6	6	6	

Separating gel for SDS-PAGE	X % gel				
Component	6	8	10	12	12
30**%** acrylamide	1.2	1.6	2	2.4	mL
4x Separating Buffer	1.5	1.5	1.5	1.5	mL
H2O	3.3	2.9	2.5	2.1	µL
10**%**APS	60	60	60	60	µL
TEMED	6	6	6	6	µL
Total	6	6	6	6	

Stacking gel	%		
Component	3.9	X	Vol.
30**%** acrylamide	0.39	X*Total/30	mL
4x Stacking Buffer	0.75	Total/4	mL
H2O	1.86	Total-A-B	mL
10**%**APS	30	Total/100	µL
TEMED	3	Total/1000	µL
Total	3	Total	mL

Lysis buffer for Phos-tag

Stock	Volume	Final Conc.
1 M Tris-HCL (pH 8.0)	1.25 ml	25 mM
0.5 M EDTA	50 µl	0.5 mM
1M DTT	0.05 ml	1mM
SDW	48.75 ml	
Protease inhibitor cocktail	1 tablet per 50 ml	
Total volume	50 ml	

Sample buffer for Phos-tag

Component	final conc.	2	4	5	Vol.
SDS	0.4%	0.40	0.80	1.00	g
1 M Tris-HCl pH 7.5	10 mM	1.00	2.00	2.50	mL
Grycerol	3%	3	6	7.5	g
BPB	0.02	0.02	0.04	0.05	g
H2O		up to Total	up to Total	up to Total	µL
Total		50	50	50	mL

5 mM Phos-tag solution		
Stock	Volume	Final conc.
Phos-Tag (AAL-107)	10 mg	5 mM
Methanol	100 µl	3%
SDW	3.2 ml	
Total volume to	3.3 ml	

10 mM $MnCl_2$		
Stock	Volume	Final conc.
Manganese (II) Tetra hydrate	1.25 ml	0.125 M
10% SDS	4 ml	4%
Sucrose	1 g	10 %
Total volume	10 ml	

30% Acrylamide solution		
Stock	Volume	Final conc.
Acrylamide	145 g	29 %
N,N'-Methylene is(acrylamide)	5 g	1%
Total volume	500 ml	Stored at 4^oC

4X Stacking Buffer (pH 6.8)		
Stock	Volume	Final conc.
Tris Base	7.2 g	120 mM
SDS	1 g	0.2 %
Adjust pH 6.8 with HCl (Hydrochloric acid)		
Total volume to	250 ml	

4X Separating Buffer (pH 8.8)		
Stock	Volume	Final conc.
Tris Base	96.9 g	1.6 M
SDS	2 g	0.4 %
Adjust pH 6.8 with HCl (Hydrochloric acid)		
Total volume to	500 ml	

10X SDS PAGE running buffer		
Stock	Volume	Final conc.
Tris Base	30 g	250 mM
Glycine	144 g	1.92 M
SDS	10 g	10%
Total volume to	1000 ml	

10X Native PAGE buffer		
Stock	Volume	Final conc.
Tris Base	15.14 g	250 mM
Glycine	72.07 g	1.92 M
Total volume to	500 ml	

10 mM EDTA Transfer Buffer		
Stock	Volume	Final conc.
10X Native PAGE buffer	50 ml	1X
Methanol	100 ml	20
0.5 EDTA	10 ml	10 mM
SDW	340 ml	
Total Volume	500 ml	

Transfer Buffer		
Stock	Volume	Final conc.
10X Native PAGE buffer	50 ml	1X
Methanol	100 ml	20
SDW	350 ml	
Total Volume	500 ml	

10X TBS		
Stock	Volume	Final conc.
Tris Base	30 g	250 mM
NaCl	90 g	1.54 M
Total Volume	1000 ml (Autoclave 121^{o}C, 15 min)	

1X TBS-T		
Stock	Volume	Final conc.
10X TBS	100 ml	1X
SDW	900 ml	1
Tween 20	1 ml	0.1 %
Total Volume	1000 ml (Autoclave 121^{o}C, 15 min)	

TBS for ChIP		
Stock	Volume	Final conc.
1 M Tris-HCL (pH 7.4)	2 ml	20 mM
5 M NaCl	3 ml	150 mM
SDW	95	
Total Volume	100 mL	